



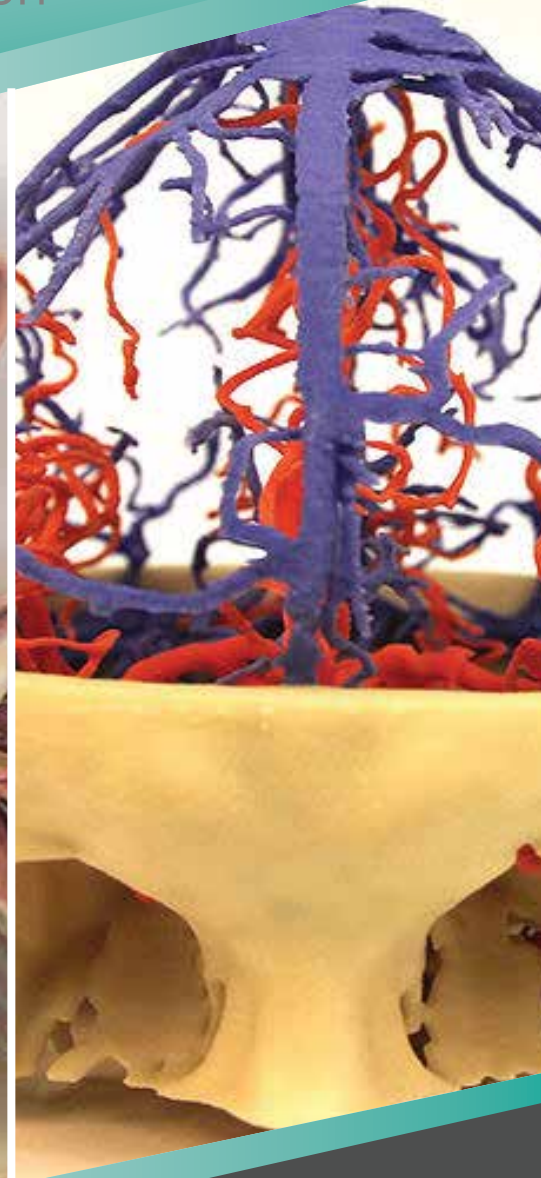
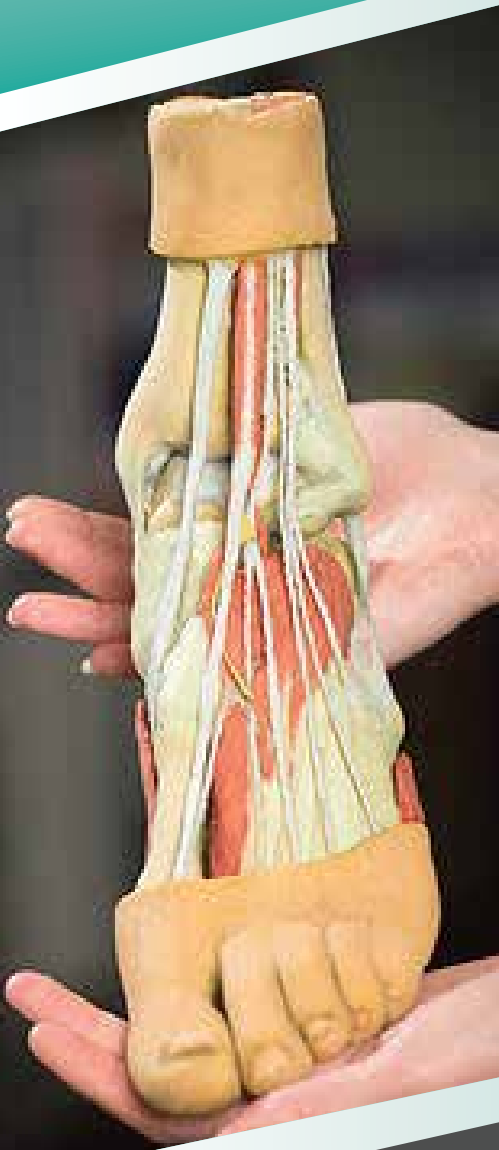
MONASH University



MENTONE
EDUCATIONAL
ANATOMICAL MODELS AND EDUCATIONAL SUPPLIES

3D Printed Anatomy Series

Human Anatomy Reproductions
with an extra dimension



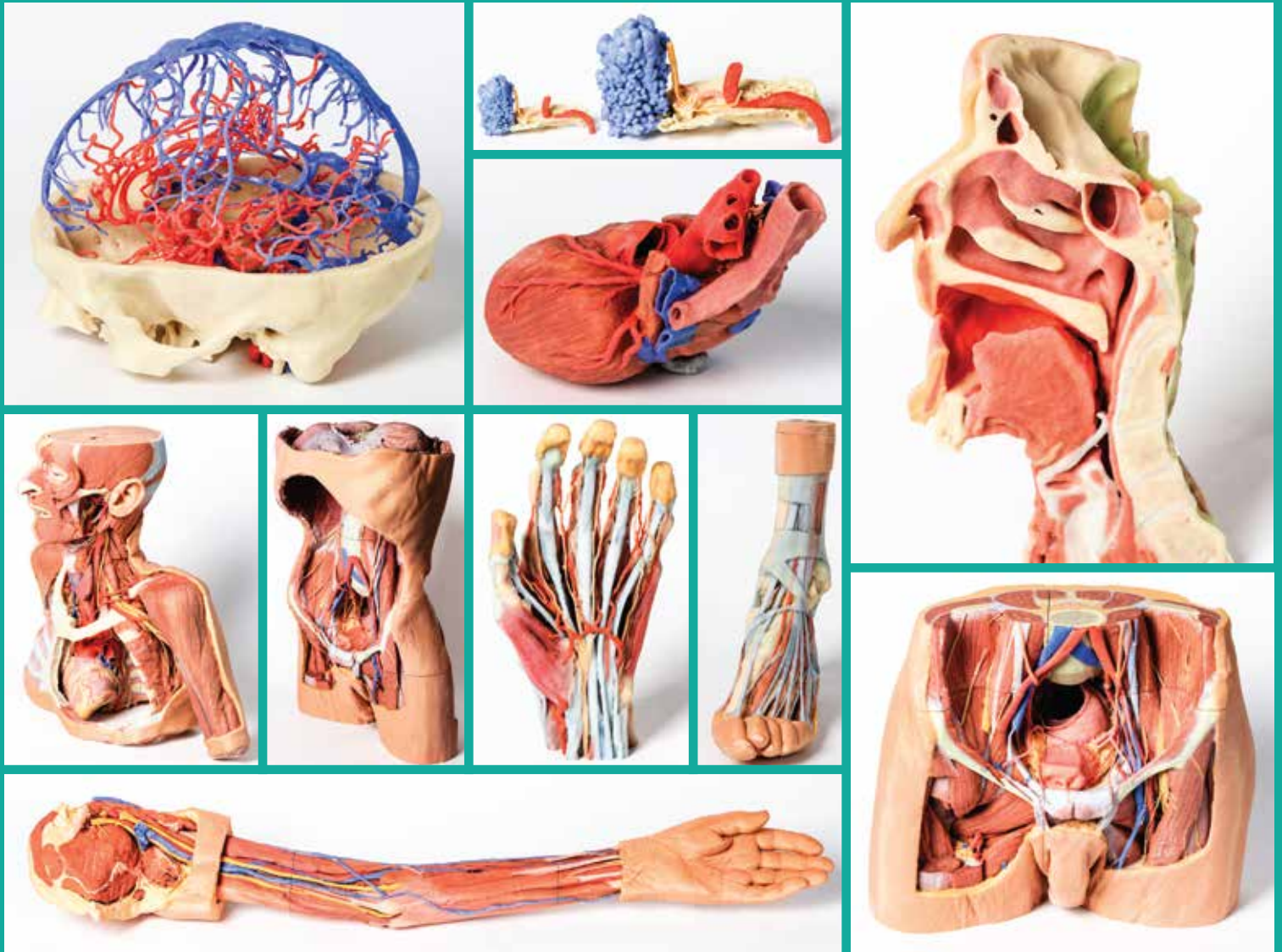
Mentone Educational
Ph: (03) 9553 3234 | Fax: (03) 9553 4562
sales@mentone-educational.com.au
www.mentone-educational.com.au

1-2	Head Neck Shoulder with angiosomes MP1250	14-15	Temporal Bone Model, Set of 3 MP1620
3	Posterior Abdominal wall MP1300	16	Paranasal Sinus model MP1630
4	Upper Limb MP1500	16	Arterial and Venous Circulation MP1640
5	Upper Limb - Arm, Forearm and Hand MP1510	17	Venous Circulation MP1645
6	Upper Limb - biceps, bones and ligaments MP1515	17	Arterial Circulation MP1650
7	Upper Limb Ligaments MP1520	18	Head and Neck MP1660
8	Right thoracic wall, axilla, and the root of the neck MP1521	19	Deep Face MP1665
9	Shoulder (left) Superficial muscles & axillary/brachial artery MP1523	20	Head and visceral column of the neck MP1670
10	Shoulder MP1525	21	Superior Orbit MP1675
11	Shoulder - deep dissection of a right shoulder girdle MP1527	22	Lateral Orbit MP1680
12	Hand Anatomy MP1530	22	Medial Orbit MP1685
13	Circle of Willis MP1600	23	Bronchial Tree MP1690
13	Dural Skull MP1610	24	Heart MP1700

24	Heart and the distal trachea, carina and primary bronchi MP1710	36	Knee Joint Extended MP1805
25	Heart internal structures MP1715	37	Flexed knee joint deep dissection MP1807
26	Bowel - Portion of Ileum MP1725	38	Lower limb musculature MP1810
26	Bowel - Portion of Jejunum MP1730	39	Lower Limb - deep dissection of a left pelvis and thigh MP1813
27	Cubital Fossa MP1750	40	Lower Limb superficial veins MP1815
28	Cubital Fossa - muscles, large nerves and the brachial artery MP1755	41	Popliteal Fossa distal thigh and proximal leg MP1820
29	Male left pelvis and proximal thigh MP1765	42	Popliteal Fossa MP1830
30	Male Pelvis MP1770	43	Foot - Structures of the plantar surface MP1900
31	Female left pelvis and proximal thigh MP1780	44	Foot - Plantar Surface and superficial dissection on the dorsum MP1910
32-33	Female right pelvis - superficial and deep structures MP1783	45	Foot - Superficial and deep dissection of the distal leg and foot MP1920
34-35	Female right pelvis MP1785	46	Foot - Superficial and deep structures of the leg and foot MP1930
36	Flexed knee joint MP1800	47	Foot - Deep plantar structures MP1940

3D Printed Anatomy Series

Advantages of 3D Printed Anatomy Series



The ground-breaking Monash 3D Printed Anatomy Series represents a unique and unrivalled collection of colour-augmented human anatomy 3D prints designed specifically for enhanced teaching and learning.

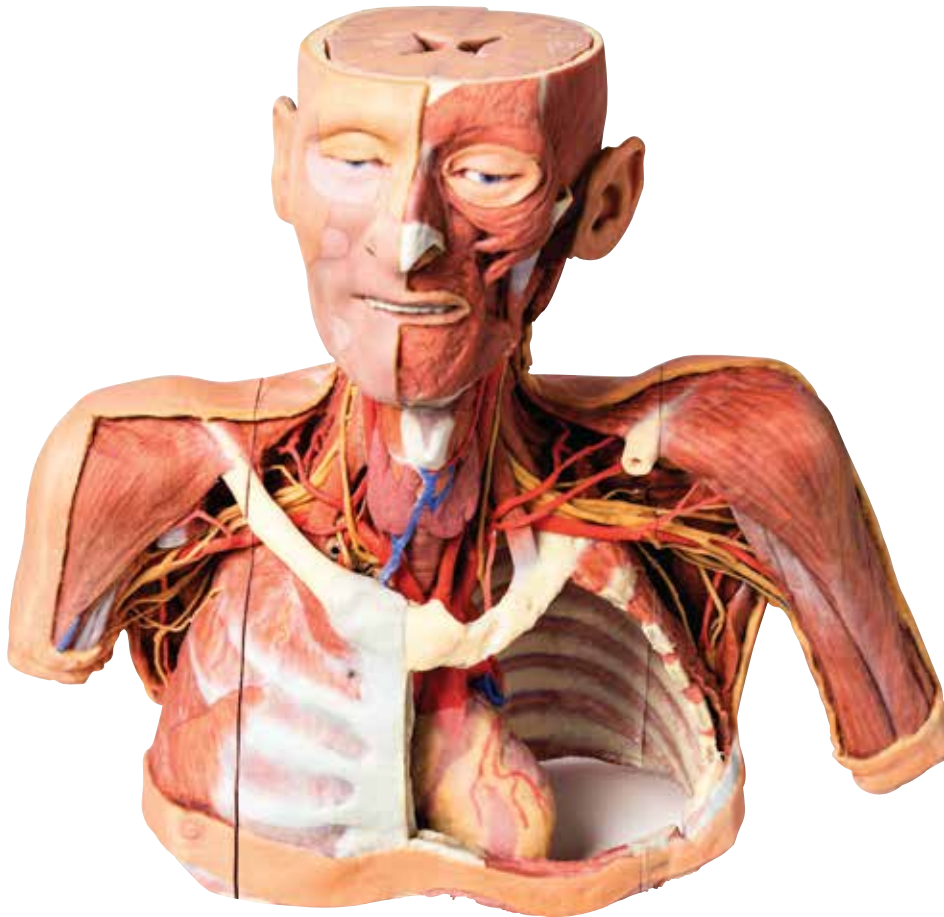
This premium collection of highly accurate normal human anatomy models has been generated directly from either radiographic data or actual cadaveric specimens using advanced imaging techniques and state-of-the-art 3D printing technology. The Monash 3D Printed Anatomy Series provides a cost effective means to meet your specific educational and demonstration needs in a range of curricula from medicine, allied health sciences and biological sciences.

What advantages does The Monash 3D Printed Anatomy Series offer over either plastic models or plastinated human specimens?

Each 3D print has been carefully reproduced from specifically selected radiographic patient data or high quality real human prosected cadaver specimens to illustrate a range of clinically important areas of anatomy with a quality and fidelity that is not possible in conventional models – this is real anatomy and not stylised.

Each 3D print has been rigorously checked by a team of highly qualified anatomists at The Centre for Human Anatomy Education, Monash University, to ensure the anatomical accuracy of the final product

The 3D prints are not real human tissue and therefore not subject to any barriers of transportation, importation or use in educational facilities that do not possess an anatomy license. The Monash 3D Printed Anatomy Series avoids these and other ethical issues that are raised when dealing with plastinated human remains.



This large, multipart 3d printed specimen displays a great deal of anatomy spanning the head, neck, thorax, axillae and upper limbs.

Head and neck: The head and neck of the specimen provides views of both superficial and deep structures in the region. The calotte has been removed ~2cm superior to the orbits to expose the brain in relation to the endocranial cavity. The transverse section through the cerebrum demonstrates the relation of the grey matter cortex to the white matter medulla, as well as the lateral ventricles with a small amount of choroid plexus visible in the base of both spaces. The skin and superficial fascia on the right side has been retained and false-coloured to display the angiosomes of the face and posterior neck. On the left side, the superficial tissues have been dissected to expose the muscles of facial expression, muscles of mastication, and deeper structures of the infratemporal fossa including the lingual nerve, terminal branches of the external carotid artery into the superficial temporal and maxillary arteries.

The carotid sheath has been opened on both sides of the neck, and the internal jugular veins and sternocleidomastoid muscles largely removed, to expose the pathway of the common carotid arteries, internal and external carotid arteries, and the vagus nerves. On the right side, the great auricular nerve ascends towards the face, while the hypoglossal nerve can be seen adjacent to the exposed stylohyoid ligament and supra- and infrahyoid muscles. A large thyroid gland is present bilaterally inferior to the thyroid cartilage, with a well-preserved superior thyroid artery and inferior thyroid vein on the right side and across the midline.

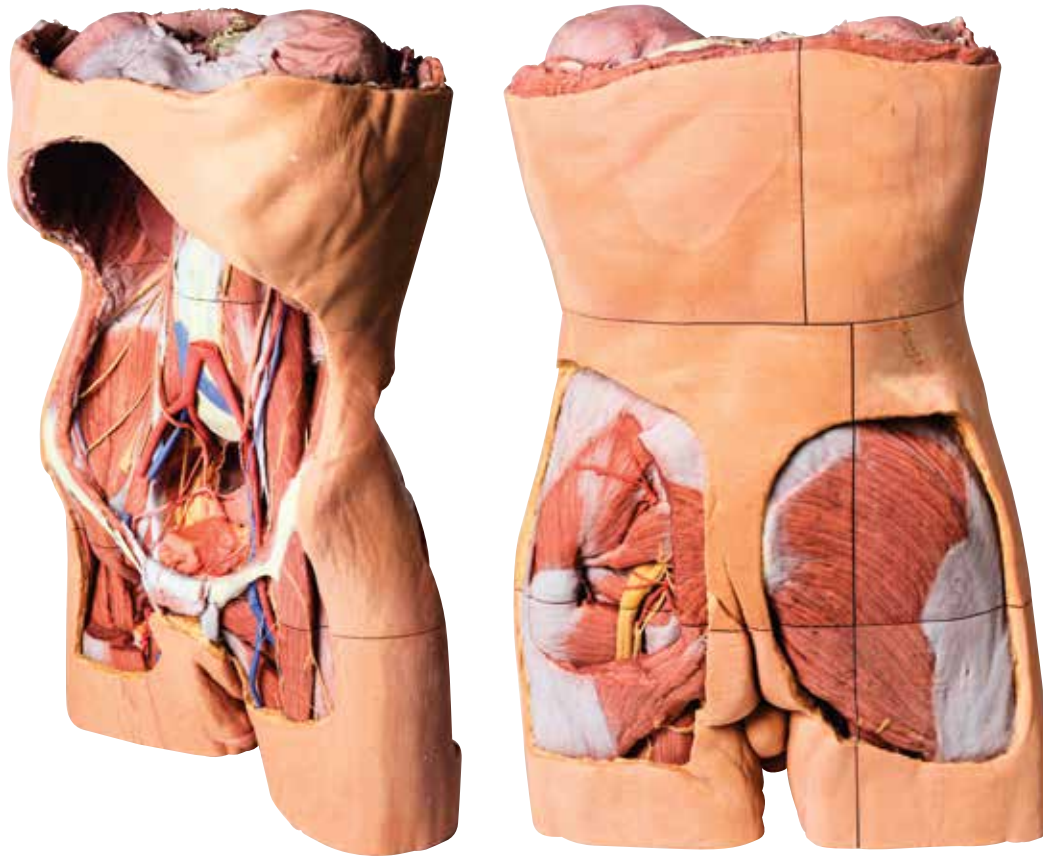
The root of the neck – axillary junction: The clavicle has been partially removed on the left side of the specimen (medial to the origin of the deltoid) to expose the first rib and the insertion of anterior scalene muscle. The roots of the brachial plexus (C5-T1) can be seen forming the trunks posterior to this muscle but anterior to middle and posterior scalene muscles they emerge from the interscalene plane. While the subclavian vein has been removed, the subclavian artery is also seen passing behind the scalenus anterior. The transition of the subclavian artery to the axillary artery is exposed, as is its position relative to the cords of the brachial plexus (medial, lateral and posterior).



The left axilla has been dissected to expose the divisions and cords of the brachial plexus and its major and minor branches. The contributions from the medial and lateral cords coming together around the axillary artery to form the median nerve is very distinctive. The course of the medial cord, the ulnar nerve, is clearly visible as is the musculocutaneous nerve as the continuation of the lateral cord. The axillary nerve is seen wrapping posteriorly around the surgical neck of the humerus. The thoracodorsal nerve and artery are seen descending on the medial wall of the axilla to enter the latissimus dorsi muscle. The long thoracic nerve is seen just anterior to this upon the serratus anterior muscle which it supplies.

The axilla/root of neck junction on the right is similar except the clavicle (and subclavius muscle) has been retained, which gives an appreciation of the dimensions of the cervico-axillary canal through which structures gain entry to the axilla. Also on the right side the pectoralis minor and major (that comprise the anterior axillary wall) have been reflected with only a small portion of their insertions being retained.

Thorax: The thorax has been opened via a 'window' on the left to display the internal thoracic wall and mediastinum. The left lung has been removed and the intercostal spaces are discernable deep to the parietal pleura although intercostal neurovascular bundles are only discernable posteriorly. The pericardium has been removed to expose the heart with its apex pointing inferiorly, anteriorly, and to the left. The left side of the heart is exposed as are the left pulmonary veins and arteries (above left main bronchus), ascending aorta, aortic arch and commencement of the descending thoracic aorta. The left vagus nerve and left recurrent laryngeal nerve are easily identified. The right half of the anterior and lateral thoracic wall are intact and display the muscles of the intercostal spaces and inserting hypaxial muscles from the right upper limb. If the specimen is viewed from below, the right lung and pleural spaces along with the diaphragmatic surface of the heart are all evident. While the skin and superficial fascia posterior thorax has been left intact, the distribution of cutaneous branches of dorsal rami have been illustrated along the left side of the specimen.



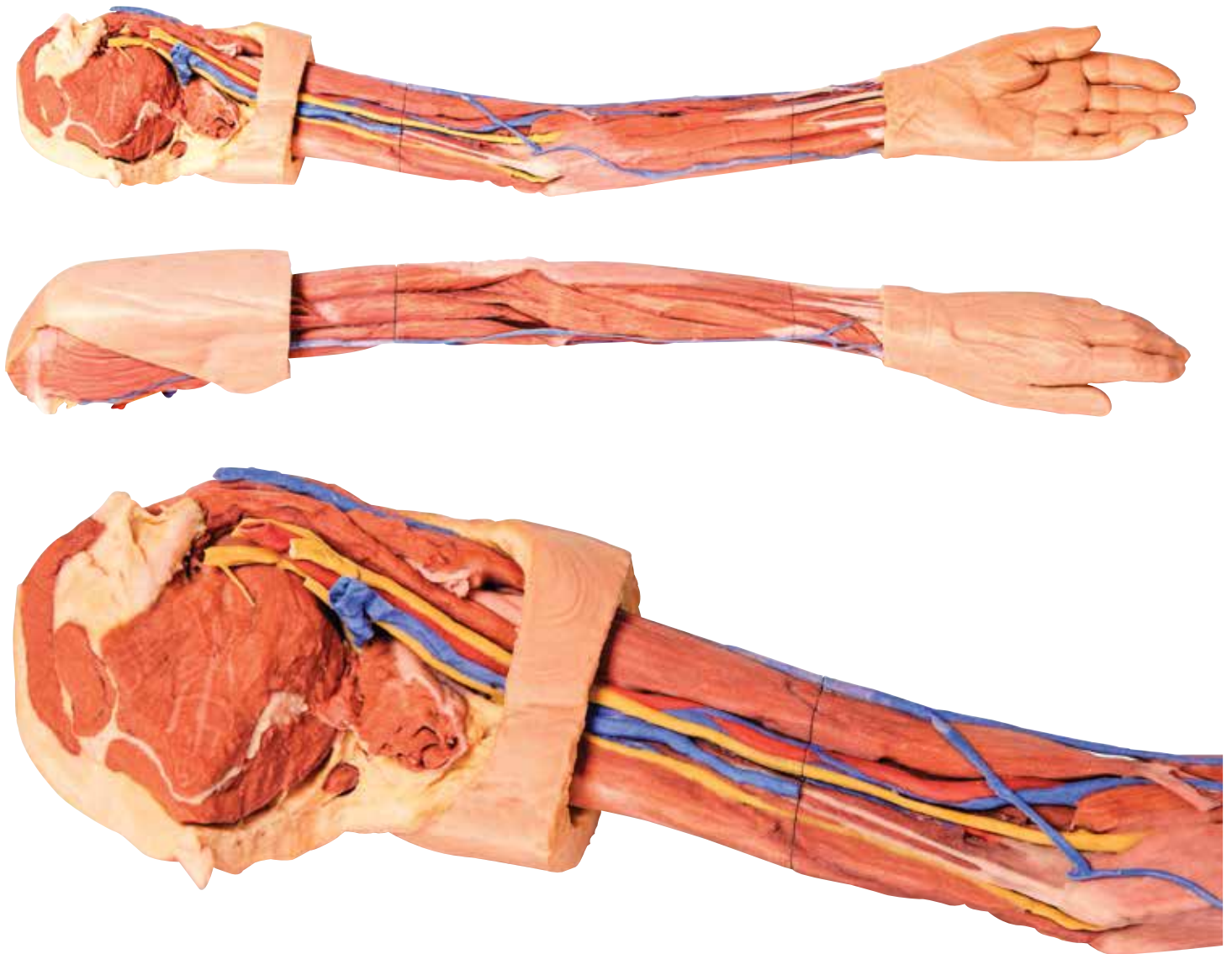
This large, multipart 3d printed specimen displays the entire male posterior abdominal wall from the diaphragm to the pelvic brim, as well as pelvic anatomy and to the proximal thigh. This same individual specimen is also available as a pelvic and proximal thigh specimen (Mp 1770).

The parietal peritoneum has been removed from the posterior abdominal wall to expose the muscular wall including the psoas, the quadratus lumborum, transversus abdominis, and the iliacus below the iliac crest. The muscular portions of the dome shaped diaphragm are clearly distinct from the central tendon. The fibres originate from the circumference of the internal walls of the bony thorax at its margin (sternal fibres, costal portion, lumbar portion). The origins of the diaphragm and the left and right crura are clearly identifiable originating from the vertebral bodies (L1-L3 on the right and L1-L2 on the left). The crura are connected by a tendinous band, the median arcuate ligament, which arches in front of the aorta; however in this specimen the aorta has been removed. The fibres of the diaphragm arising from the tendinous arches over psoas and the lateral arcuate ligaments are partly hidden by the kidneys. The oesophageal opening through the arching fibres of the right crus is present above (level of T10) and to the left of the aortic opening (level of T12). The opening in the central tendon that transmits the inferior vena cava (level of T8/9 intervertebral disc).

The somatic nerves of the posterior abdominal wall are clearly identifiable and consist of from above downwards – the subcostal, the iliohypogastric and ilioinguinal nerves lie on the quadratus lumborum (in this individual they arise together and– this can often occur and they split later in abdominal muscle layers), the lateral cutaneous nerve of thigh, the femoral lying in the groove between psoas and iliacus), and the genitofemoral nerve lying superficially upon psoas. The sympathetic trunks can be seen descending lateral to the lumbar vertebral bodies.

The aorta and inferior cava are transected around the level of L3 vertebral body. The aortic bifurcation into the right and left common iliac arteries is slightly higher than normal.

Finally, the kidneys have dissected from the peri- and pararenal fat of the posterior abdominal wall. The renal vessels (arteries anteriorly, veins posteriorly) have been preserved but as the aorta and inferior cava have been removed this does display the origin and arrangements of these vessels fully. The more inferior position of the right kidney is clearly visible and the ureters can be seen emerging from the hilum and descending initially lateral to psoas, then anterior to this muscle before crossing pelvic brim anterior to the bifurcation of the common iliac arteries to reach the true pelvis.



This 3D print demonstrates a superficial dissection of a left upper limb from the blade of the scapula to the hand. The skin, superficial and deep fascia has been removed from most of the limb except over the dorsum of the scapula, proximal arm, and over the hand. The median cubital vein, cephalic and basilic veins are preserved, with the latter two preserve from the wrist to their terminations (in the deltopectoral groove and brachial vein, respectively).

In the axilla, cross-sections of the deltoid, supraspinatus, infraspinatus, teres minor, teres major, and subscapularis muscles are visible relative to the bony blade and spine of the scapula. The coracobrachialis and tendon of the latissimus dorsi are also preserved, as well as the tendon of the pectoralis major. The lateral portions of the axillary artery and vein and the most lateral extend of the cords of the brachial plexus (medial, lateral, posterior) are also present. Terminal nerves of the brachial plexus visible in the axilla of this specimen include the upper subscapular, ulnar, median, musculocutaneous, axillary and radial.

The course of the deep vessels and nerves of the upper limb is exposed through the arm from proximal to distal, as well as the muscles of the anterior and posterior compartments. In the cubital region part of the bicipital aponeurosis is preserved. The superficial layer of anterior and posterior forearm muscles are exposed from their origin to their tendons distally, with a small portion of deep forearm fascia over the extensor compartment maintained for reference. At the most distal extent of the dissected forearm, the ulnar and radial arteries and median nerve are visible.



This upper limb specimen displays the vascular, nervous and muscular anatomy of a left distal arm, forearm and hand.

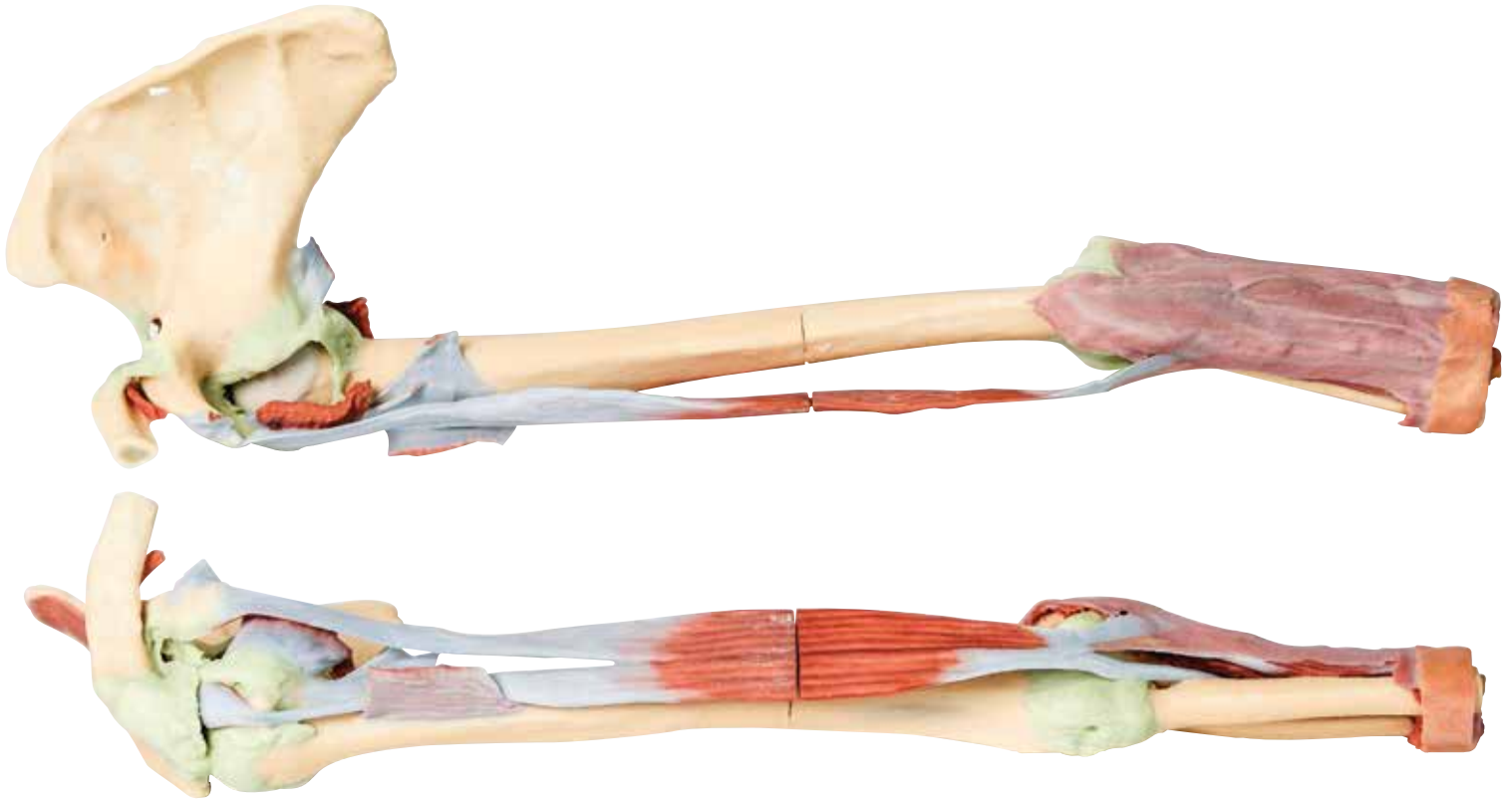
In the distal arm and elbow/cubital fossa region we can see the arrangement of the biceps tendon, brachial artery and median nerve from lateral to medial. The bicipital aponeurosis has been divided to reveal the structures deep to it. The ulnar nerve can be seen passing behind the medial epicondyle with an ulnar collateral artery close by. The superficial branch of the radial nerve can just be seen in the space between brachioradialis and brachialis muscles (as the belly of the latter muscle has been displaced slightly laterally).

In the forearm, the superficial flexor muscles arising from the common flexor origin can be clearly seen (from lateral to medial– pronator teres, flexor carpi radialis (FCR), flexor digitorum superficialis (FDS) and flexor carpi ulnaris (FCU)). There is not a palmaris longus muscle in this cadaver. The radial artery and superficial branch of the radial nerve (emerging half way down the forearm from behind the brachioradialis muscle and tendon) are clearly identifiable. The ulnar artery can be seen in the distal forearm emerging from beneath FCU muscle.

On the posterior aspect of the forearm the extensor muscles arising from the common extensor origin are clearly identifiable. These include (from medial to lateral) the extensor carpi ulnaris (ECU), extensor digiti minimi, extensor digitorum and extensor carpi radialis brevis (ECRB). The extensor carpi radialis longus (ECRL) can be seen arising from the inferior aspect of the lateral supracondylar ridge. Further distally the abductor pollicis longus (APL) and extensor pollicis brevis (EPB) can be seen emerging from deep to superficial and ‘wrapping’ around the radius. They along with extensor pollicis longus (EPL) (partly hidden) travel distally to insert into the extensor or dorsal surface of the base of the 1st metacarpal, proximal phalanx

and distal phalanx of the thumb, respectively. The anatomical snuff-box is displayed with the radial artery in its floor (surrounded by fat) and the cutaneous branch of the radial nerve in its roof. The extensor retinaculum is clearly visible on the dorsum of the wrist and distal to it the tendons of extensor indicis and ECRB and ECRL can be seen inserting into the 2nd and 3rd metacarpals.

In the hand, the superficial dissection reveals muscles of the thenar and hypothenar eminences, the flexor retinaculum of the hand (roof of the carpal tunnel), the long tendons of the hand, the lumbricals, and the superficial palmar arch arising from the ulnar artery, which passes into the hand lateral to the pisiform bone above the retinaculum, along with the superficial branch of the ulnar nerve. The large median nerve can be seen passing beneath the flexor retinaculum between the FCR and the FDS tendons. Digital arteries and nerves can be clearly seen further distally in the palm entering the digits. Note in particular the small recurrent branch of the median nerve crossing over the flexor pollicis brevis close to its origin from the retinaculum. The extensor expansion is dissected on the middle finger.



This 3D print shows the origin and insertion of biceps (most other arm and shoulder muscle bellies have been removed). The long head of biceps arises from the supraglenoid tubercle (hidden from view) and travels inferiorly in the bicipital groove, whereas the short head of biceps arises from the coracoid process. The bifid insertion of the muscle as the bicipital aponeurosis and the rounded tendon which can be seen winding around the radius to insert into the radial tuberosity are clearly discernable.

At the shoulder region the dissected attachments of some muscles (subclavius, subscapularis, pectoralis major, teres minor, infraspinatus, long head of triceps) and the tendinous insertion of latissimus dorsi can be identified close to the 'floor' of the medial lip of the bicipital groove. The tendon of teres major lies on the medial lip of the groove and the pectoralis major tendon inserts into the lateral lip of the groove. The tendon of pectoralis minor arises from the coracoid process medial to the origin of the short head of biceps. Ligaments of the shoulder region such as the coracoclavicular, coracoacromial, coracohumeral are visible, as is the glenohumeral and acromioclavicular joint capsules. The supraspinatus muscle is the only rotator cuff muscle that has been completely preserved. The suprascapular ligament which bridges across the suprascapular notch is also evident on the superior border of the scapula.

At the elbow, the capsule of the joint including the annular ligament of the radius are exposed. The radial collateral ligaments are also just discernable. The ulnar collateral ligament is not visible as the two heads of flexor carpi ulnaris have been retained.

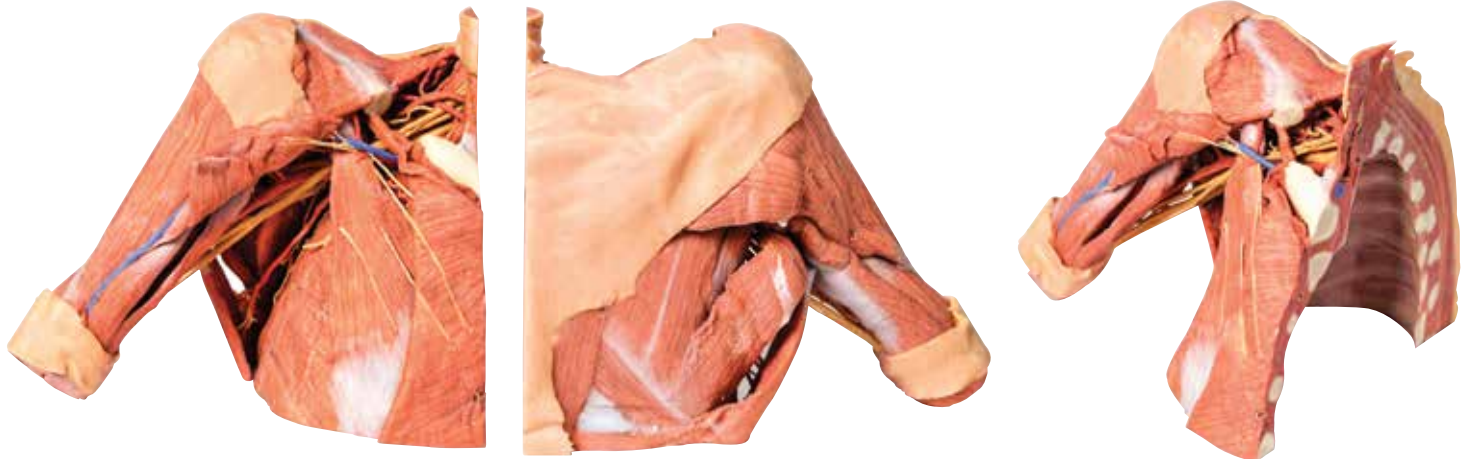


This 3D printed specimen presents the entire upper limb skeleton and ligaments from the pectoral girdle to the hand. In the pectoral girdle, the ligaments spanning the clavicle and scapula (acromioclavicular, coracoclavicular, coracoacromial) as well as the superior transverse scapular ligament spanning the suprascapular notch, are visible.

A small portion of the supraspinatus muscle belly and tendon are preserved to demonstrate the passage of the muscle deep to the coracoacromial ligament, which is a very clinically relevant area of anatomy. The tendon of the subscapularis muscle has been reflected slightly to expose the anterior aspect of the glenohumeral joint capsule, and the tendon of the long head of triceps brachii, teres major, and latissimus dorsi are preserved surrounding the capsule and proximal humerus. The tendon of the long head of biceps brachii is visible within the intertubercular groove, and exposed within the superior glenohumeral joint capsule as it approaches the supraglenoid tubercle.

The capsule of the elbow joint has been dissected to expose the articular surfaces of the distal humerus, proximal radius and proximal ulna. Both the ulnar and radial collateral ligaments are preserved, as is the annular ligament of the radius. Just distal to the joint capsule, the tendinous insertion of the biceps brachii is preserved as it inserts into the dorsal aspect of radial tuberosity.

Distal to the interosseous membrane, the palmar and dorsal ligaments of the wrist joint are preserved (including the radial and ulnar collateral ligaments, palmar and dorsal radiocarpal and ulnocarpal ligaments, pisohamate, pisometacarpal, radiate capitate, palmar and dorsal carpometacarpal ligaments). In the hand, the metacarpophalangeal and interphalangeal joint capsules with collateral ligaments are preserved for all digits, including the palmar ligaments (volar plates); the capsules are open dorsally to appreciate the articulations between elements. The terminal portions of the flexor digitorum superficialis and profundus tendons are retained to show their insertions into the bases of the intermediate and distal phalanges, as is the flexor pollicis longus tendon inserting to the base of the terminal phalanx of the first digit.



This 3D printed specimen preserves a dissection of the right thoracic wall, axilla, and the root of the neck. The specimen is cut just parasagittally and the visceral contents of the chest have been removed. Structures within the right chest wall are visible deep to the parietal pleura, including the ribs, muscles of the intercostal spaces and the origins of the neurovascular bundle in each intercostal space. The pectoralis major has been reflected medially towards the sectioned edge of the specimen to expose pectoralis minor which acts as a useful landmark as it divides the axillary artery into its three parts. The clavicle has had its middle 1/3 removed, but the subclavius muscle has been retained. The brachial plexus and many of its branches are seen almost in its entirety from the roots of C5-T1 to its termination as it exits the axilla to enter the arm. Of the structures preserved on the specimen:

Nerves: The medial pectoral nerves can be seen penetrating pectoralis minor, while the lateral pectoral nerve can be identified on the medial upper border of the pectoralis minor (one branch of which is reflected with the transected humeral portion of the pectoralis major). The cords of the brachial plexus can be identified around the 2nd part of the axillary artery. The major terminal nerves of the plexus (musculocutaneous, median, ulnar, radial and axillary nerves) are all identifiable. The long thoracic nerve is visible lying on the surface of serratus anterior, as is the thoracodorsal nerve alongside the thoracodorsal artery as they descend to enter the latissimus dorsi muscle. The dorsal scapular nerve and artery are visible above and below omohyoid. The axillary nerve accompanied by the posterior circumflex humeral artery can be seen passing posteriorly just below the neck of the humerus. At the elbow, the capsule of the joint including the annular ligament of the radius are exposed. The radial collateral ligaments are also just discernable. The ulnar collateral ligament is not visible as the two heads of flexor carpi ulnaris have been retained.

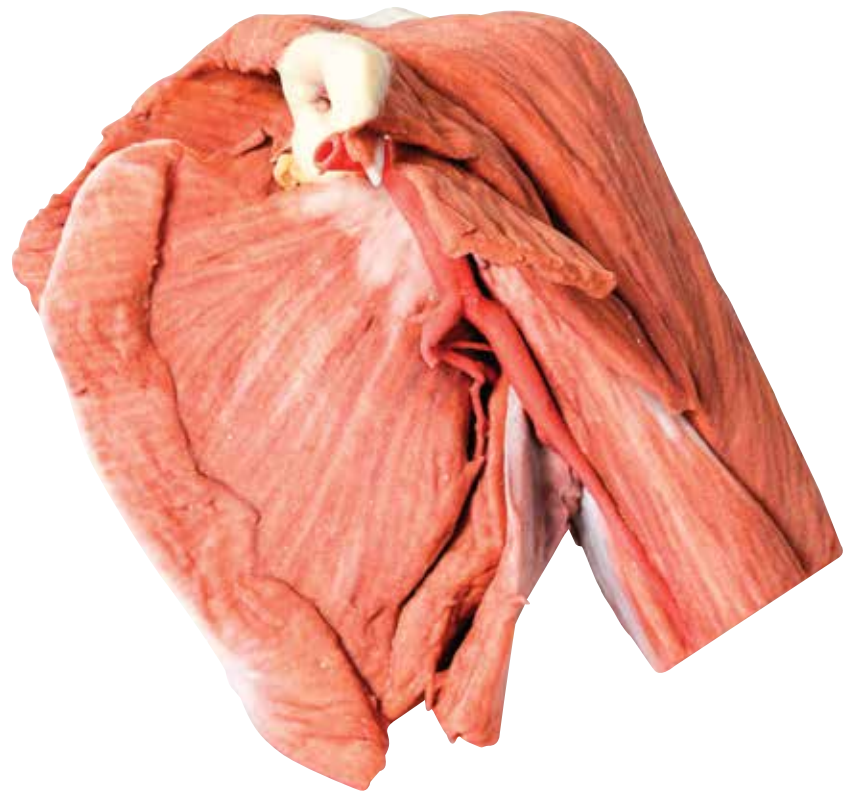
In the root of the neck the phrenic nerve is just visible as it passes on the anterior surface of scalenus anterior muscle from its lateral border to its medial border and a thin accessory phrenic nerve is identifiable.

Vessels: Some of the branches of the subclavian artery (e.g., the transverse cervical and suprascapular arteries passing transversely across the root of the neck) can be clearly seen, however the subclavian artery itself is partly hidden from view as it crosses the first rib behind the insertion of scalenus anterior muscle. Most of the deep veins have been removed to expose branches of the three parts of the axillary artery, including the thoracoacromial artery and its branches, the lateral thoracic artery, thoracodorsal artery and the anterior and posterior circumflex humeral arteries. While the deep veins have been removed the cephalic vein can be seen ascending superficially in the deltopectoral groove into the deltopectoral triangle where it passes through the clavipectoral fascia.

Muscles: The digitations of the serratus anterior muscle are clearly visible on the lateral chest wall. As mentioned above, the pectoralis major muscle is reflected to reveal the pectoralis minor which together form the anterior wall of the axilla. Posteriorly the large fan shaped latissimus dorsi is the most obvious muscle along with the teres major. When viewed posteriorly a few vertical fibers of trapezius can be seen, as can some descending fibers of the lower part of rhomboid major attaching to the medial border of the scapula. Below this the triangle of auscultation is clearly visible. The infraspinatus and teres minor muscles are also visible arising from the infraspinous fossa and lateral border of the scapula respectively. The triceps brachii muscle can be seen in the extensor compartment of the arm.

In the root of the neck the insertion of sternocleidomastoid is visible medially and the trapezius is visible posteriorly. In the floor of the posterior triangle the scalene muscles are visible as is the omohyoid as it lies obliquely in the triangle.

Shoulder (left) Superficial muscles and axillary/brachial artery MP1523



This printed 3D left shoulder specimen consists of the scapula, humerus (sectioned near midshaft) and clavicle (sectioned at midshaft) with the superficial muscles around the shoulder joint, the rotator cuff muscles and the axillary artery as it progresses distally to become the brachial artery.

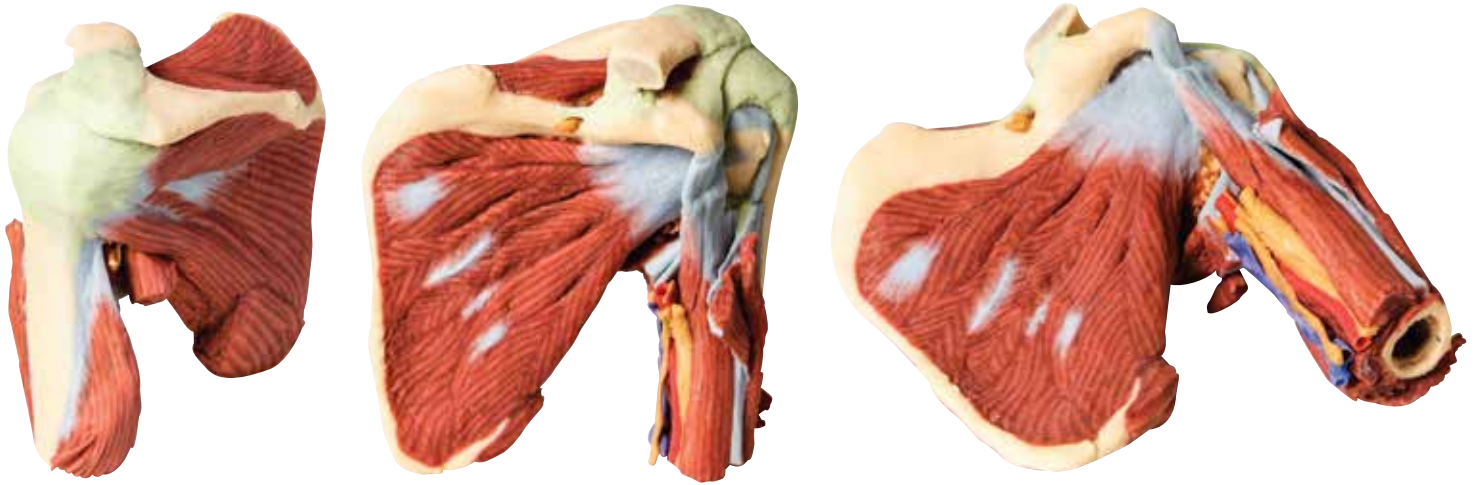
The muscles attached to the clavicle have been preserved including the subclavius muscle attachment to the inferior border of the clavicle and the deltoid covering the lateral aspect of the proximal upper limb (overlying the origins of the long head of biceps brachii and the lateral head of triceps brachii). The clavicular head of the pectoralis major has been preserved. On the posterior aspect the superior fibers of trapezius can also be observed where they attach to the posterior border of the lateral third of the clavicle, and to the acromion process and the spine of the scapula. Other muscles attached to the scapula which have been preserved include the subscapularis and serratus anterior on the anterior or costal aspect. Inspection of the anterior aspect reveals that the pectoralis minor insertion onto the coracoid process of the scapula has been preserved. Posteriorly the teres major and teres minor muscles are clearly visible arising from the lateral border of the scapula. Supraspinatus is preserved but infraspinatus has partly been removed to show branches of the suprascapular artery passing from the suprascapular fossa around the base of the spine to enter the infraspinous fossa housing the infraspinatus muscle. A small part of the omohyoid attachment is also visible above the suprascapular ligament.

The axillary artery below the inferior border of the clavicle can be seen to give off the thoracoacromial branch anteriorly and just slightly more distally the suprascapular artery can be seen passing posteriorly. Coursing distally, it gives off posterior branches of the circumflex scapular and subscapular arteries. The anterior and posterior circumflex humeral arteries are hidden from view when viewed from in front, however the latter artery can be seen deep to the posterior fibres of deltoid as it emerges through quadrangular space. Below the inferior border of teres major the axillary artery becomes the brachial artery. The radial collateral artery is visible arising from the brachial artery. The axillary artery becomes the brachial artery beyond the lower margin of the teres major muscle. The muscles of the proximal upper limb have all been preserved, and those of the superficial layer, i.e. long head of biceps brachii, and long and lateral heads of triceps brachii, can be observed to form a complete layer of musculature around the humerus. The cross section of the mid shaft of the humerus nicely displays the relations of the major neurovascular bundles and the muscles in the anterior and posterior compartments.

A small remnant of the suprascapular nerve passing under the suprascapular ligament is visible.

3D Printed Anatomy Series

Shoulder - deep dissection of the left shoulder joint, musculature, and associated nerves and vessels MP1525



This 3D printed specimen presents a deep dissection of the left shoulder joint, musculature, and associated nerves and vessels of the scapula and proximal humerus (to near midshaft). Anteriorly, the deltoid muscle has been detached from its origin to expose the underlying deeper structures of the shoulder joint and rotator cuff musculature. The suprascapular nerve and artery are visible passing deep to, and superficial to, the superior transverse scapular ligament respectively. The multipennate subscapularis muscle is fully exposed with its tendinous insertion visible deep to the short head of the biceps brachii muscle. The insertion of the deltoid is preserved just overlying the long head of the biceps brachii, which ascends through the bicipital groove towards the glenohumeral joint capsule.

Adjacent to the short head of the biceps brachii is the neurovascular bundle of the brachial artery, brachial vein, and terminal nerves of the brachial plexus (radial, ulnar, median, and the medial antebrachial cutaneous). The tendon of the latissimus dorsi, teres major, teres minor and long head of the triceps brachii muscles have been cut enhance the visibility of the medial aspect of the humerus, including the passage of the axillary nerve into the quadrangular space, the origin of the profunda brachii artery accompanying the radial nerve, and the insertion of the short head of the triceps brachii muscle. On the posterior aspect, the infraspinatus and supraspinatus muscles are fully exposed from their origins to insertions on the proximal humerus. The glenohumeral joint capsule is intact, with the extracapsular ligaments (e.g., acromioclavicular, coracoacromial, and coracoclavicular [both conoid and trapezoid portions]) preserved.

3D Printed Anatomy Series

Shoulder - deep dissection of a right shoulder girdle, preserving a complete scapula, lateral clavicle, and proximal humerus MP1527



This 3D printed specimen preserves a deep dissection of a right shoulder girdle, consisting of a complete scapula, lateral clavicle, and proximal humerus. In the anterior view, the subscapularis muscle is present but sectioned to highlight the cross-sectional thickness of the belly within the subscapular fossa.

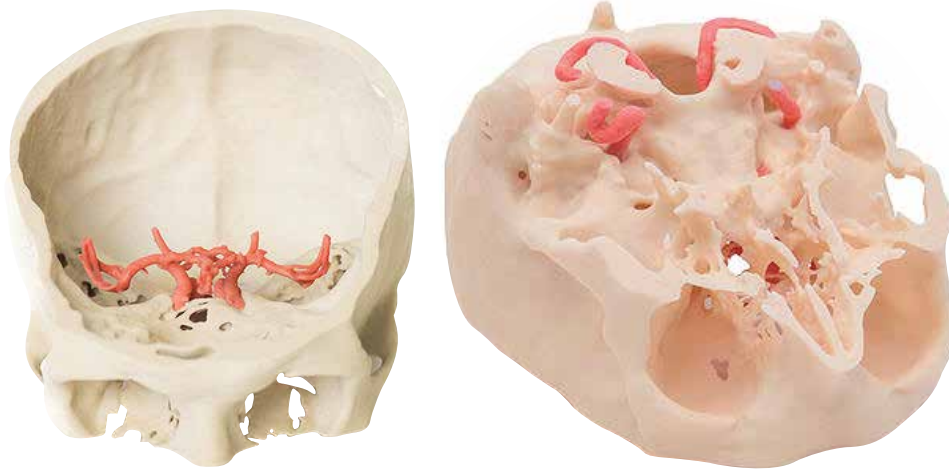
The coracoclavicular ligament and coracoacromial ligaments lie just medial to the insertions of the coracobrachialis and pectoralis minor muscles on the coracoid process of the scapula. The insertion of the tendon of the latissimus dorsi is covered by the tendon of the long head of the biceps brachii muscle passing in the bicipital groove towards the glenohumeral joint capsule. The capsule has been opened anteriorly to expose the passage of this tendon, as well as the suprapinatus muscle (covered by the collapsed subdeltoid bursa). In the posterior view the supraspinatus muscle is preserved while the infraspinatus and teres muscles have been removed to expose the posterior glenohumeral joint capsule. The terminal insertions of the long head of the triceps brachii, infraspinatus, and teres minor muscles are all preserved.



This 3D printed specimen demonstrates a superficial dissection of a left hand and wrist. Anteriorly, the transverse carpal and palmar carpal ligaments have been removed to expose the tendons and nerves traversing the carpal tunnel and Canal of Guyon.

The palmar aponeurosis has been removed to demonstrate the course of the tendons through the palm, the superficial muscles of the thenar and hypothenar eminences (abductors and flexors), and the lumbrical muscles arising from the flexor digitorum tendon. In the digits, the fibrous sheaths have been removed to expose the flexor pollicis longus tendon and the spatial relationships between the flexor digitorum superficialis and profundus tendons as they insert into the intermediate and terminal phalanges. Also visible in the midpalm is the superficial palmar arch with contributions from superficial branches of the ulnar and radial arteries. The superficial palmar arch branches (common palmar) and terminal arteries (proper palmar digital) are visible to the terminal phalanges. Accompanying these vessels are the corresponding common and proper palmar digital nerves from the median and ulnar nerves. Also visible in the wrist are the tendons of the flexor carpi radialis and flexor carpi ulnaris tendons, and the radial and ulnar arteries.

Posteriorly, the radial artery can be seen traversing the floor of the anatomical snuffbox and giving rise to both the deep branch (piercing the first dorsal interosseous muscle) and the dorsal carpal branch. The superficial fascia and extensor retinaculum has been removed to display the course and insertions of the extensor muscle tendons, as well as the tendons of the extensor pollicis longus, brevis, and abductor pollicis longus muscles. Both intertendinous connections and the extensor expansions (with insertions from the first dorsal interosseous and lumbrical) visible.



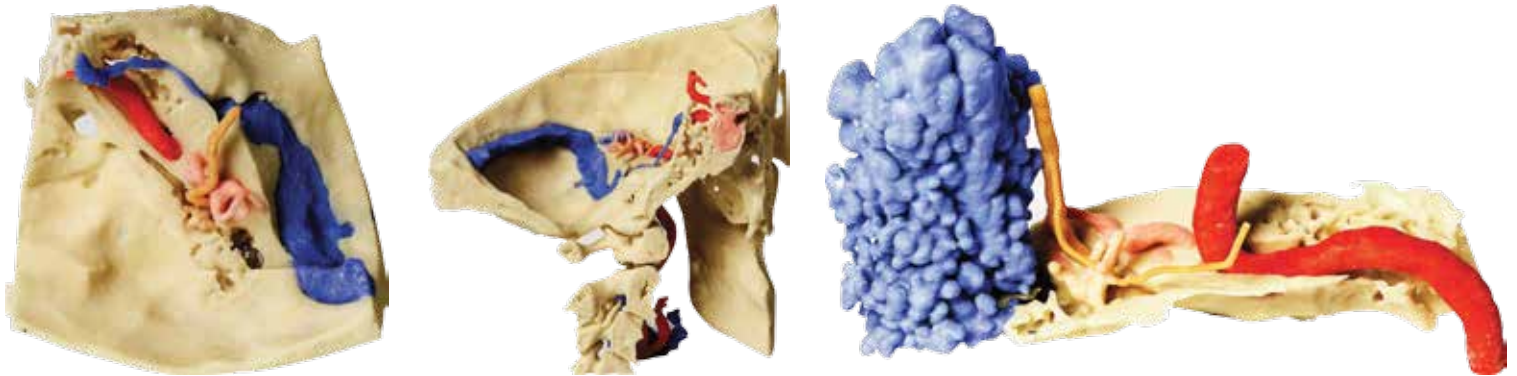
This 3D printed specimen demonstrates the intracranial arteries that supply the brain relative to the inferior portions of the viscerocranium and neurocranium. This print was created by careful segmentation of angiographic data. The model shows the paired vertebral arteries entering the cranial cavity through the foramen magnum and uniting to form the basilar artery. The basilar can be seen dividing into their terminal posterior cerebral arteries. The superior cerebellar arteries arise just proximal to this termination.

The internal carotid arteries (ICAs) can be traced from the point where they enter the petrous portion of the temporal bone via the carotid canal and travel medially and anteriorly to emerge on the superior margin of the foramen lacerum. It is here that each ICA lies within the cavernous sinus (not shown). The S-shaped carotid siphon on both left and right sides are most beautifully demonstrated lateral to the sella turcica. The ICAs then pass medial to the anterior clinoid processes. We note that (as in up to 30% of individuals) there has been ossification of the ligamentous bridge between the middle clinoid processes and the anterior clinoid process to create a caroticoclinoid foramen. The ICAs then divide into anterior and middle cerebral arteries. The paired posterior communicating arteries are clearly visible connecting the posterior cerebral and middle cerebral arteries. The completion of the Circle of Willis, made by the single anterior communicating artery between the anterior cerebral arteries is difficult to discern as the anterior cerebral arteries lie so close together.



This 3D print of a dissected and opened cranial cavity displays the dural folds and dural venous sinuses, including the falx cerebri (preserved by a retained midsagittal portion of the calvaria). The intact tentorium cerebelli demonstrates the tentorial notch which normally houses the midbrain.

Across the dural folds the following sinuses are visible (light blue coloring): superior sagittal sinus, inferior sagittal sinus, straight sinus, transverse sinuses, superior and inferior petrosal sinuses, sphenoparietal sinuses and the cavernous sinuses. In the region of the sella turcica, the entry of the carotid arteries to the cranial cavity through the roof of the cavernous sinuses is also visible.



This 3 part 3D printed model derived from CT data highlights the complex anatomy of the temporal bone including bone ossicles, canals, chambers, foramina and air spaces. In addition, the spatial relations between temporal bone and other structures of otological importance, i.e. carotid artery, dural venous sinuses, related nerves and the dura mater are indicated. Internal casts (endocasts) of the bony chambers and canals have been created to aid visualisation of the internal anatomy of the temporal bone

Part 1 Skull Preparation

The specimen has been trimmed to reveal the posterior quadrant of the left side of the skull including the posterior (cerebellar part only) and middle cranial fossa. The model shows the location of the temporal bone and its relationship with the adjoining sphenoid, parietal and occipital bones. The superior aspect of the petrous part of the temporal bone including the tegmen tympani has been removed to reveal its detailed internal architecture, and structure associated with the auditory and vestibular apparatus. The middle ear (coloured orange) is revealed to show the tympanum, along with the aditus, antrum (laterally), and the 'bone' part of the pharyngotympanic tube and the bony canal of the tensor tympani muscle (medially). Collectively, these form a direct anterior-posterior passage between the nasopharynx and the mastoid air cells (coloured blue). The anatomical position of the incus relative to the tympanic membrane can be seen via the external auditory meatus. The bony labyrinth of the vestibular apparatus of the inner ear (green) is seen juxtaposed with the middle ear.

The orthogonal arrangement of the anterior, lateral, and posterior semicircular canals and the spiral organisation of the cochlea can be clearly identified. The passage of the facial nerve (CN VII) through the petrous part of the temporal bone and its intimate spatial relationship with the auditory and vestibular apparatus is shown in yellow. Proximad, the nerve courses in an anterolateral direction before descending distally to emerge from the bone via the stylomastoid foramen located between the mastoid and styloid processes. The condyle of the mandible can be seen in the mandibular fossa at the origin of the zygomatic process of squamous part of the temporal bone. The temporomandibular joint has had the capsule removed to reveal the articular disc of the joint (indicated by a blue/grey colouration). The anterior aspect of the mastoid process has been transected to show the extensive nature of the mastoid air cells. The cervical part of the internal carotid artery can be seen ascending to enter into the carotid canal within the petrous part of the temporal bone. Its anteromedial course can be seen within the exposed aspect of the bone, and its s-shaped continuance within the cavernous sinus of the sphenoid bone, and its emergence into the neurocranium. The model also shows the transverse dural venous sinus, its continuation into the sigmoidal sinus (located on the posterior internal aspect of the squamous part of the temporal bone), and passage through the jugular foramen to form the internal jugular vein. The inferior petrosal sinus is also seen leading into the jugular foramen. The model also shows the foramen magnum and first three cervical vertebrae cut in parasagittal section. Note the sphenoid sinus located axially within the base of the sphenoid bone (coloured blue)

Part 2 The Petrous Part Of The Temporal Bone

This model is derived from the overall skull preparation and has been enlarged (x3) to further illustrate the detailed internal architecture of the petrous part of the temporal bone and the auditory and vestibular apparatus. As in Part 1 internal casts of the bony labyrinth of the inner ear, mastoid air cells, and the bony canal of the internal carotid artery are used to aid comprehension of this complex and important region.

The bony ossicles of the middle ear (incus, malleus and stapes) are shown within the middle ear cavity, and the bony prominence of the lateral semicircular canal of the vestibular apparatus can be seen protruding into the middle ear. The connection from the tympanum or middle ear to the mastoid air cells (Blue) via the aditus and antrum is visible.

The model also shows the facial nerve entering the internal acoustic meatus on the anterior aspect of the petrous bone. The chorda tympani is seen branching from the facial nerve in its descending portion in the facial canal. This small nerve, which carries parasympathetic fibres and taste fibres to the anterior 2/3 of the tongue, can be seen passing through the tympanic cavity between the incus and malleus. The bone canal of the tensor tympani muscle can be seen extending away from the tympanic cavity of the middle ear.

Part 3 The Auditory And Vestibular Apparatus

As in Part 2, this model has been enlarged (x3) to highlight the detailed internal architecture of the auditory and vestibular apparatus and its relationship to anatomical features of otological importance. The petrous part of the temporal bone and tegmen tympani have been removed to expose the tympanum, aditus and antrum of the tympanic cavity of the middle ear. The model shows the direct connection between nasopharynx and mastoid air cells via the bony canal of the pharyngotympanic tube. The ossicles of the middle ear are seen within the tympanum or middle ear.

The model also shows the bony labyrinth of the vestibular apparatus of the inner ear, and the tympanic prominence of the lateral semicircular canal can be seen within the tympanum of the middle ear.

The passage of the facial (CN VII) and vestibulocochlear (CN VIII) nerves through the petrous part of the temporal bone, and their intimate spatial relationship with the auditory and vestibular apparatus is shown in yellow. The cochlear nerve is seen entering the cochlear region of the bony labyrinth of the inner ear. The genu and geniculate ganglion of the facial nerve are shown immediately before the facial nerve descends within the facial canal, to emerge via the stylomastoid foramen located between the mastoid and styloid processes. The chorda tympani is seen within the tympanum of the middle ear, passing between the incus and malleus. The emergence of the chorda tympani is shown from the petrotympanic fissure, located medial to the mandibular fossa of the temporal bone.

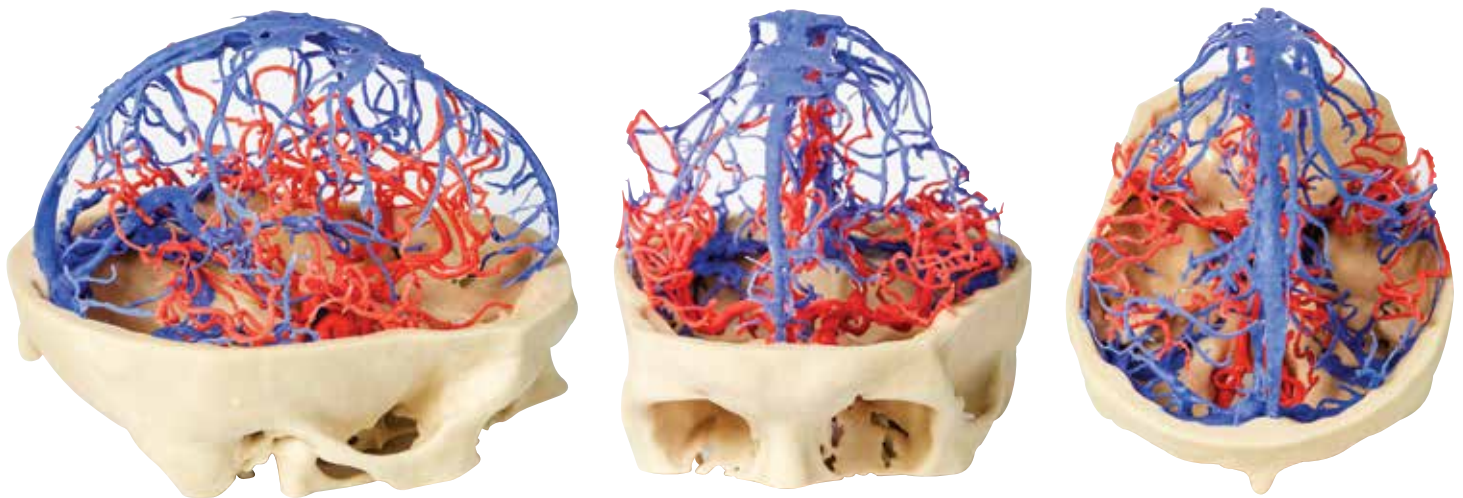
Paranasal Sinus model MP1630



This unique model has been created from CT imaging and segmentation of the internal spaces of the viscerocranium. Parts of the skull have been retained but sections or windows have been removed to expose the paranasal sinuses.

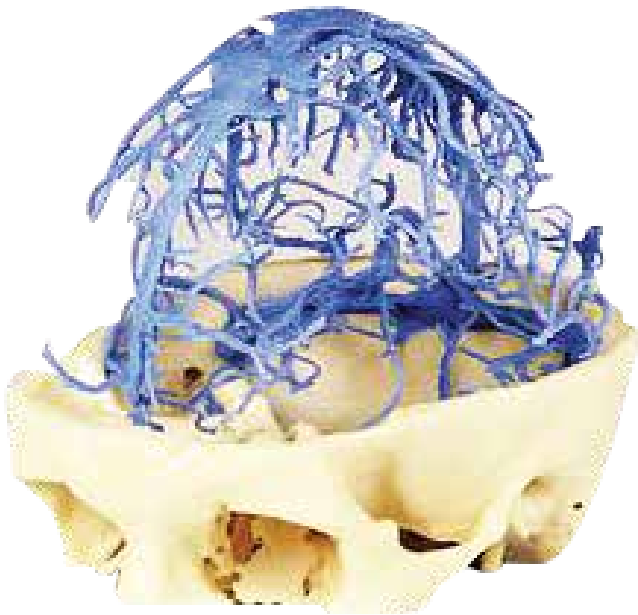
The paired frontal sinuses, with the right being partially subdivided, are coloured blue. The left frontal sinus is largely surrounded by frontal bone, while the right is completely exposed and shows the frontonasal ostium which drain as a funnel shaped tube into the infundibulum of the middle meatus of the nasal cavity. The ethmoid sinuses or air cells, coloured purple, are only shown on the left. The medial wall of the orbit composed of the orbital plate of the ethmoid bone is retained. The maxillary sinus (green) on the left has been partly exposed and partly left within the maxilla. The opening of the maxillary sinus into the lateral wall of the nose is barely discernable as a small green patch in the middle meatus. The left sphenoid sinus (pink) is also displayed, within the opened sphenoid bone.

Arterial and Venous Circulation MP1640



This 3D printed specimen integrates segmented angiographic data of both the cranial arterial and venous circulation into a single model. Further description of the visible structures can be found under the 'Circle of Willis', 'Cranial Arterial Circulation' and 'Cranial Venous Circulation' prints.

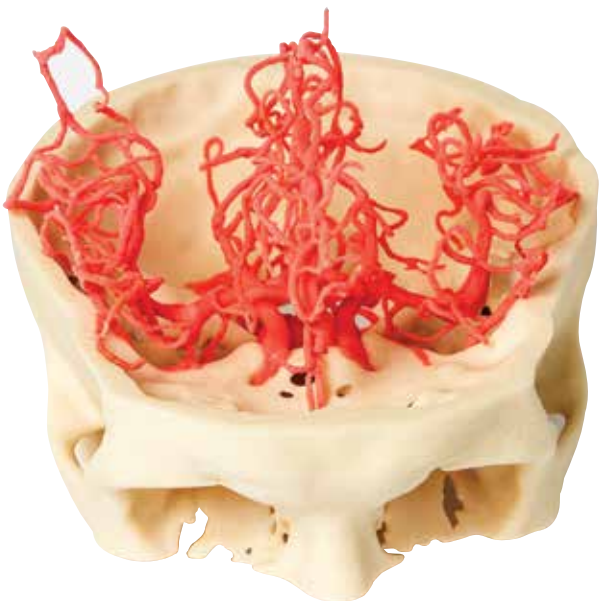
Venous Circulation MP1645



This 3D print presents the same dataset that underlies our Circle of Willis and cranial arterial circulation 3D prints and is derived from careful segmentation of angiographic data.

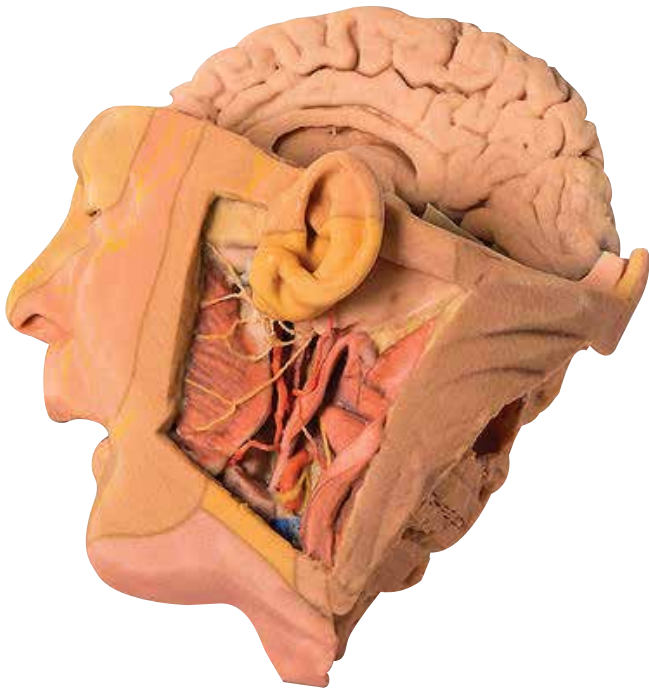
Here, the dural venous sinus network has been segmented based on structures visible from the circulation of contrast medium in the late phase of filling. As a result, while most of the sinuses are present, the lack of contrast in the anterior portions of the venous system means that some structures are not as clear in the model as may be expected – for example the cavernous sinus and inferior petrosal sinus. The extensive network of dural veins and venous lacunae are visible, which drain towards the midline in the superior sagittal sinus. Deep to this network of sinus veins are the great cerebral vein which drains with the inferior sagittal sinus into the straight sinus which then converges with the superior sagittal at the confluence of sinuses. Several dural veins drain into the left and right transverse sinuses as they pass anteriorly towards the petrous portion of the temporal bone. The sigmoid sinuses can be seen in the posterior cranial fossa prior to exiting the skull at the jugular foramen and forming the internal jugular vein (visible on the inferior surface of the skull).

Arterial Circulation MP1650



This 3D print presents an expanded version of the same dataset that underlies our Circle of Willis 3D print derived from careful segmentation of angiographic data.

Like our Circle of Willis print, this model demonstrates the internal carotid and vertebral arteries entering the skull, branching into the intracranial arteries that supply the brain. This more expanded 3D print of the internal carotid and vertebral artery and their branches, inclusive of the Circle of Willis, displays the full branching pattern of the cerebral and cerebellar arteries. This includes the pericallosal arteries (from the anterior cerebrals) with its named branches, the superior and inferior divisions of the middle cerebral (including sulcal, temporal, and parietal arteries), and the posterior cerebral artery branches. The ophthalmic artery can also be seen as the first intracranial branch of the internal carotid artery entering the optic canal.



This 3D printed specimen of a parasagittally sectioned head and neck demonstrates a range of anatomical features:

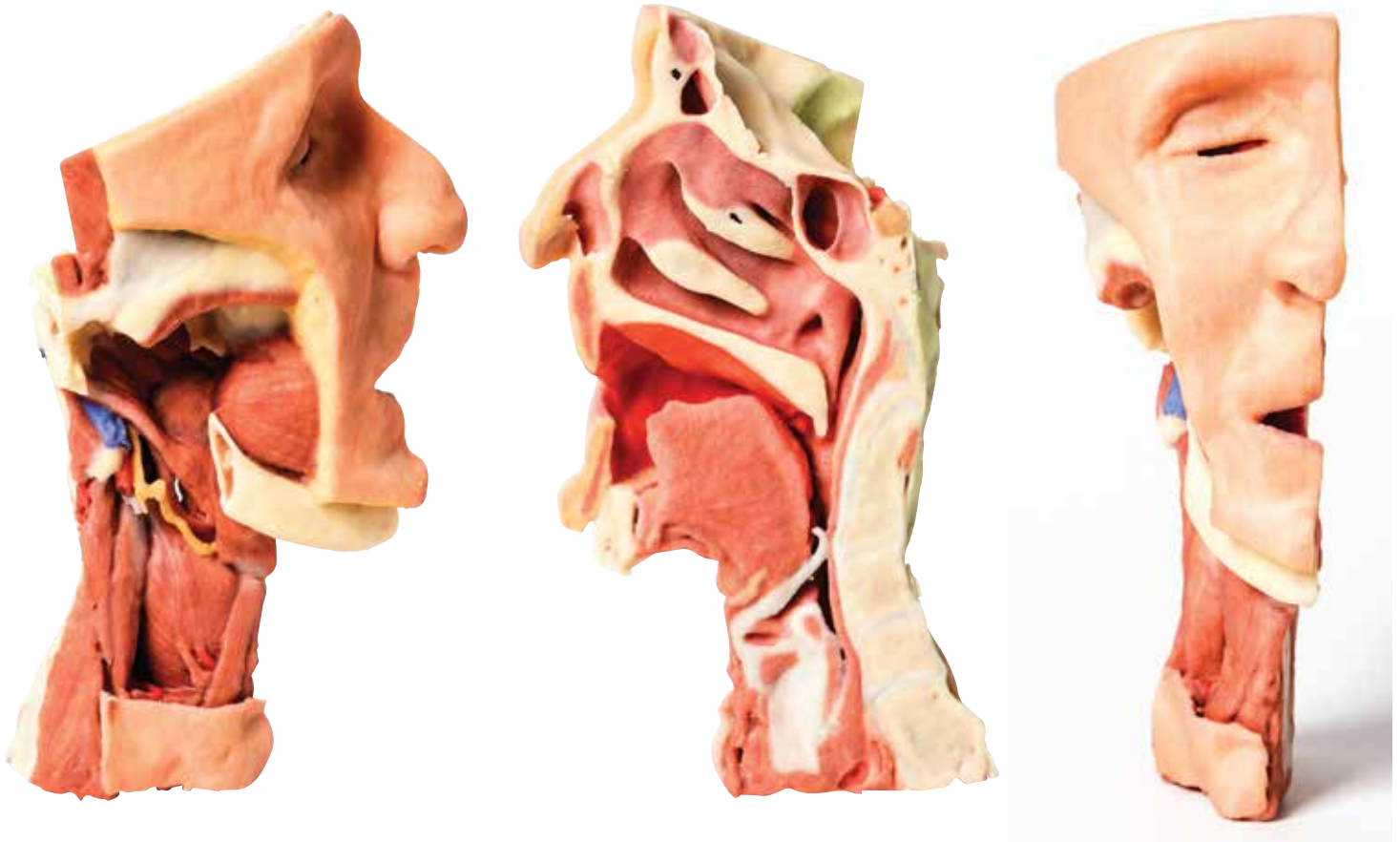
Lateral aspect of the face: A window has been created to expose the parotid region. The pinna of the ear has been left intact, however the mastoid process has been exposed by reflection of the sternocleidomastoid (SCM) muscle. The parotid gland has been carefully removed to display structures which are normally embedded or hidden by the gland. The attachment of the posterior belly of digastric arising from the digastric groove medial to the mastoid process can be clearly seen. The masseter muscle is identifiable as it inserts into the lateral surface of the ramus and angle of the mandible. The condyle of the mandible can be seen in an opened temporomandibular joint (TMJ). The articular disc of the TMJ is indicated by a blue/grey colouration. The external carotid artery (ECA) can be seen passing deep to the digastric muscle and tendon. The branches of the ECA including facial artery, the maxillary artery, occipital artery and posterior auricular artery are preserved. At the inferior aspect of the dissected window one can see the cut remains of the internal jugular vein (IJV) and the cut upper surface of the submandibular gland and the hypoglossal nerve winding around the ECA on its lateral surface. The vagus nerve is just visible between the ECA/common carotid and the IJV. Emerging posterior to digastric one can see the spinal part of the accessory nerve superficial to the levator scapulae muscle (stretched due to the manner in which the SCM has been reflected).

The facial nerve can be seen emerging from the stylomastoid foramen immediately posterior to the styloid process and dividing into temporal, zygomatic, buccal and marginal mandibular branches on the face.

The branches of the trigeminal that supply the dermatomes of the face are illustrated diagrammatically by painted nerves on the skin of the face.

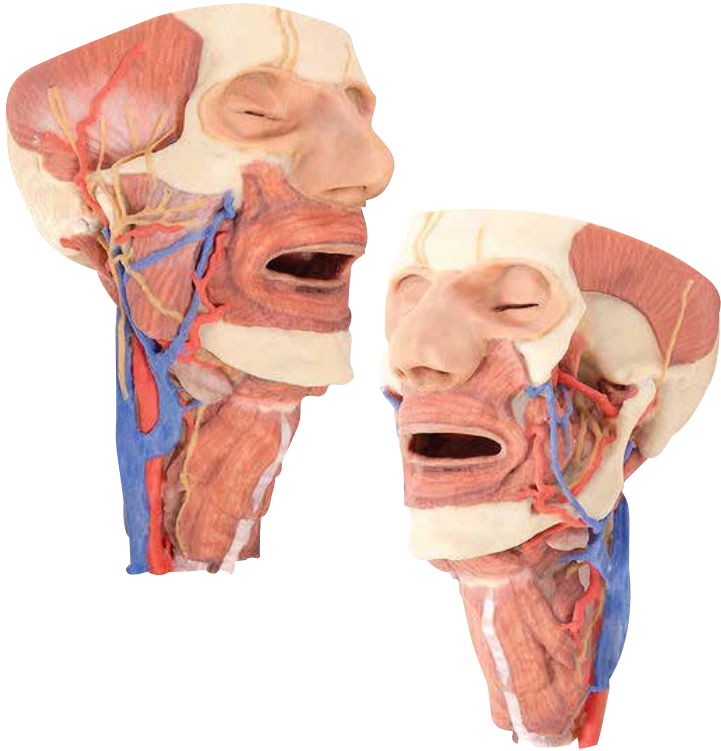
Brain and cranial cavity: The medial surface of the cerebrum with the corpus callosum and thalamus are demonstrated. The septum pelucidum has been removed. The left hemisphere of the cerebellum and cerebral hemispheres have been removed to expose the floor of the left anterior, middle and posterior cranial fossa and the fourth ventricle. The anatomy around the cavernous sinus and sella turcica is well displayed. The intracranial course of cranial nerves II, III, V, VII, VIII, IX, X and spinal part of XI are also highlighted from their origin from the brainstem. The facial canal has been opened by removal of part of the temporal bone to expose the facial nerve, the geniculate ganglion and its course in the middle ear (due to removal of the tegmen tympani).

Medial surface: The parasagittal cut surface shows the lateral ventricle, the right cerebral peduncle, posterior cerebral artery, and the cut edge of the tentorium cerebelli. In the region of the sphenoid the internal carotid artery and the carotid siphon are visible in the cavernous sinus as it pierces the dural roof (pale green) to commence its intracranial course. Here it lies lateral to the right optic chiasm. The mouth, tongue, associated muscles, lateral aspect of the nasal cavity, nasopharynx, and cut muscles and vertebrae are also visible on the medial surface of this parasagittal section.



In this 3D printed specimen of a midsagittally-sectioned right face and neck, the ramus, coronoid process and head of the mandible have been removed to expose the deep part of the infratemporal fossa. The pterygoid muscles have also been removed to expose the lateral pterygoid plate and posterior surface of the maxilla. The buccinator has been retained and can be seen originating from the external aspect of the maxilla, the pterygomandibular raphe and the external aspect of the (edentulous) mandible. The superior constrictor can also be seen arising from the posterior aspect of the pterygomandibular raphe. The internal laryngeal nerve has been preserved. Muscles in the neck that are identifiable include mylohyoid, the strap muscles and the inferior constrictor. The styloid muscles can be seen descending from the process to their insertions (not shown). The internal carotid artery can be seen deep to the styloid process which gives origin to stylohyoid, styloglossus and stylopharyngeus.

The sectioned surface preserves a series of midline head and neck structures, including: the lateral wall of the nasal cavity (superior, middle and inferior conchae and sphenoidal recess, superior meatus, middle meatus and inferior meatus), the nasopharynx, the opening of the auditory tube, the hard palate, soft palate, the intrinsic tongue muscles, oropharynx, laryngopharynx, and hyoid bone. The parts of the laryngeal cartilages and the pharynx are clearly seen, as are the vertebral bodies of C2-C5, the anterior arch of C1 (atlas), and the dens of C2 (axis).



This 3D print specimen preserves a series of features of the head and visceral column of the neck:

The face: On the right side of the head the parotid gland has been removed to reveal the facial nerve and all its branches (temporal, zygomatic, buccal, marginal mandibular and cervical) and demonstrate the spatial relations of structures embedded in the gland from superficial to deep (facial nerve, retromandibular vein, external carotid artery). In the surrounding region the temporalis, masseter and posterior belly of digastric are exposed, as are and the facial artery, transverse facial artery and superficial temporal artery. The facial vein and transverse facial vein are clearly visible uniting to form the common facial vein which is joined by the retromandibular vein to form the external jugular vein.

Viewed from the anterior aspect the face has been dissected to display some of the facial muscles around the mouth (buccinator [on the left], orbicularis oris and zygomaticus major). On the left side of the infratemporal fossa has been open to expose the medial and lateral pterygoids. The lateral pterygoid is divided to show the mandibular division of the trigeminal nerve dividing into the lingual nerve and the inferior alveolar branch. Also on the left side the branches of the ophthalmic division of the trigeminal that supply the skin above the eyebrows and scalp (supraorbital [left only] and supratrochlear nerves [both sides]) are dissected. The submandibular gland is clearly visible below the mandible on both sides as are the facial arteries and veins as they course over the mandible.

The neck: The musculoskeletal portion of the neck have been removed to display the pharynx posteriorly, the larynx anteriorly, and the neurovascular bundles laterally. The suprahyoid and infrahyoid muscles can be seen on the neck, as well as the cricothyroid muscle. When looking up the length of the trachea from below, the vocal folds are visible. The hypoglossal nerve can be seen winding around the lateral surface of the external carotid artery and the external branch of superior laryngeal nerve is seen descending in the neck. The internal jugular vein, the common carotid artery and its bifurcation into external and internal carotid arteries are clearly seen on both left and right. The vagus nerve in the carotid sheath is also visible. The ansa cervicalis is visible emerging below the digastric muscle and descending on the surface of the internal jugular vein. The internal branch of the superior laryngeal nerve can be seen below the superior thyroid artery on the left. The superior thyroid artery branching from the external carotid artery is seen descending in the anterior neck. The internal branch of the superior laryngeal artery is visible on the left piercing the thyrohyoid membrane above the inferior constrictor where this muscle is attached to the hyoid bone.

Posterior view of the pharynx: The superior, middle and inferior pharyngeal constrictors are indicated on the pharynx wall. The oesophagus can be identified emerging from the lower end of the pharynx. The posterior horn of the hyoid bone acts as a useful landmark. The carotid sheath seen from behind clearly shows the vagus nerve and its pharyngeal branches on the left. The recurrent laryngeal nerve is briefly visible on the left lying medial to the inferior thyroid artery. The occipital arteries are visible as they curve around the mastoid process. The vertebral arteries are seen either side of the brainstem as they enter the foramen magnum. The cerebellum has been removed to allow the fourth ventricle to be exposed. The cut surfaces of the cerebellar peduncles are clearly visible. A large portion of the posterior inferior cerebellar artery on the right is still visible as it winds around around the brainstem.

Cranial Cavity: The left and right orbits have been opened to reveal the orbital nerves and vessels along with the eyes and optic nerves. The optic chiasm, optic tracts and the lateral geniculate bodies are retained thus showing a large part of the visual pathways. The brainstem is cut at the level of the superior colliculi on the left and slightly lower on the right. The olfactory tracts and bulbs are also demonstrated. The origins of many of the cranial nerves from the brainstem are clearly visible.



This 3D printed model captures a dissection in which the calvaria and cerebrum have been removed to expose the floors of the anterior and middle cranial fossae. The midbrain has been sectioned at the level of the tentorium cerebelli and on the cross sectional surface one can identify the superior colliculi, cerebral peduncles and the substantia nigra. Anterior to the mid-brain the vertebral artery can be clearly identified rising from the posterior cranial fossa and dividing into the posterior cerebral arteries. Anterior to this in the region of the sella turcica one can identify the internal carotid arteries emerging from the roof of the cavernous sinus medial to the anterior clinoid processes and beneath and lateral to the optic nerves and chiasm. The oculomotor nerves are visible penetrating the roof of the cavernous sinuses on the left and right posterior to the point where the internal carotid arteries emerge.

Anteriorly in the midline of the anterior cranial fossa lies the crista galli with the olfactory bulbs still present above the cribriform plates on either side. On the right the orbital plate of the frontal bone (the roof of the orbit) has been removed to expose the frontal nerve splitting into the supraorbital and supratrochlear nerves lying superior to the levator palpebrae superioris. The trochlear nerve is visible entering the superior aspect of the superior oblique muscle belly on the medial aspect of the orbit. Ethmoidal air cells have been exposed in the medial orbital wall by removal of the part of the lamina papyracea. On the left the levator palpebrae and superior rectus muscles have been divided along with the frontal nerve to expose the optic nerve, nasociliary nerve, ophthalmic artery and superior ophthalmic vein in the intraconal space. The face has been dissected to show facial muscles around the orbit on the right and the infraorbital nerve on the left. The infratrochlear nerve is also shown on the right and facial veins and arteries are also visible.

Lateral Orbit MP1680



This 3D printed specimen shows the orbit from the lateral perspective when the bony lateral wall and part of the calvaria of the skull have been removed.

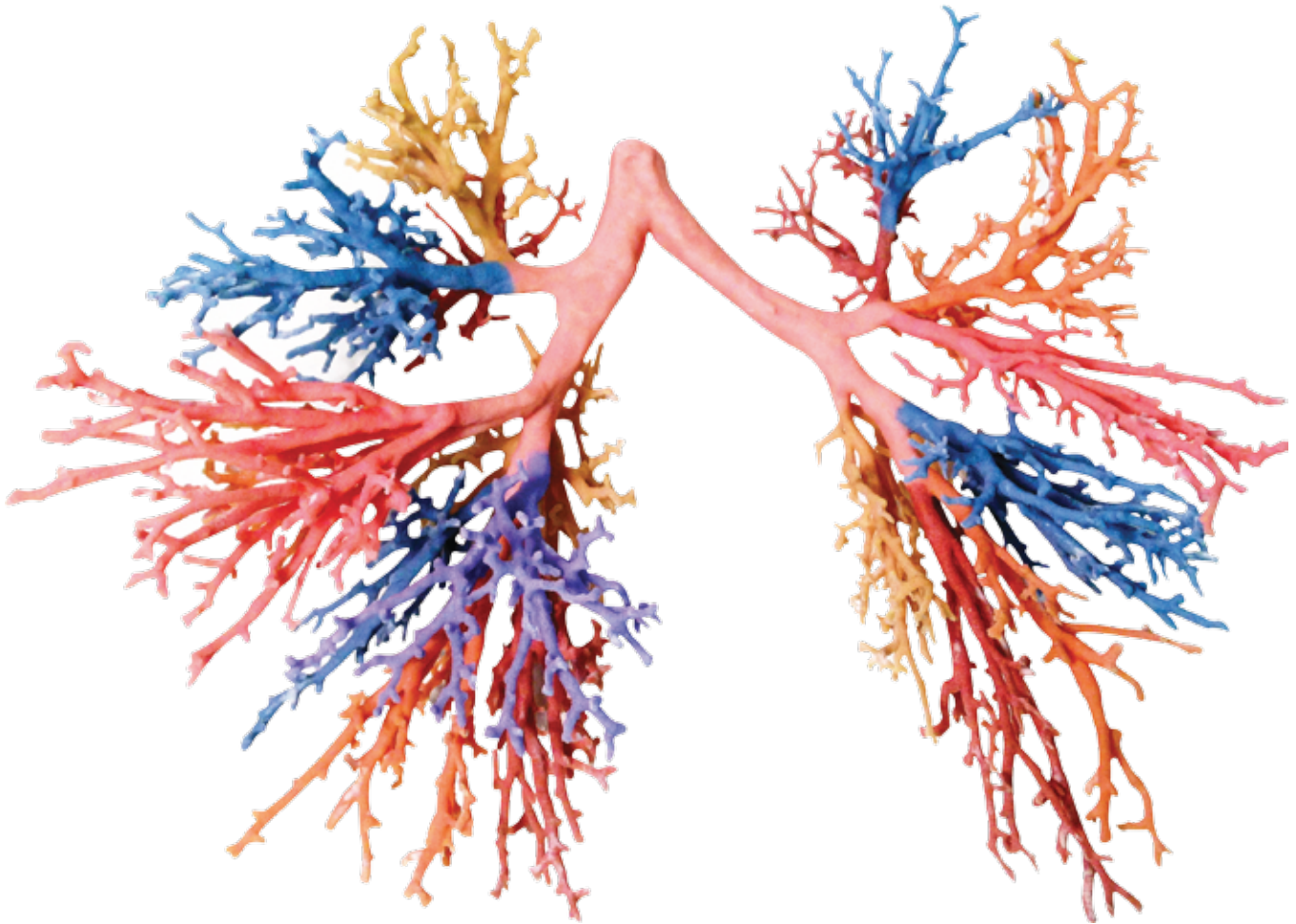
The frontal and temporal lobes of the brain are exposed. In the orbit the lateral rectus (LR) has been divided to demonstrate the intracranial space. The muscle near its insertion has been reflected anteriorly to reveal the insertion of inferior oblique muscle (IO). The portion near its origin from the annulus is reflected to reveal the abducens nerve (VI Nv) entering the bulbar aspect of the muscle belly. Other features shown include the tarsal plate (TP), lacrimal gland (LG), the lacrimal artery (LA) and lacrimal nerve (LNv) and numerous other nerves and vessels around the optic nerve.

Medial Orbit MP1685



This 3D print displays the orbital contents and its close relations as viewed from the medial perspective when the majority of the lateral wall of the nasal cavity and the intervening ethmoidal sinuses have been removed.

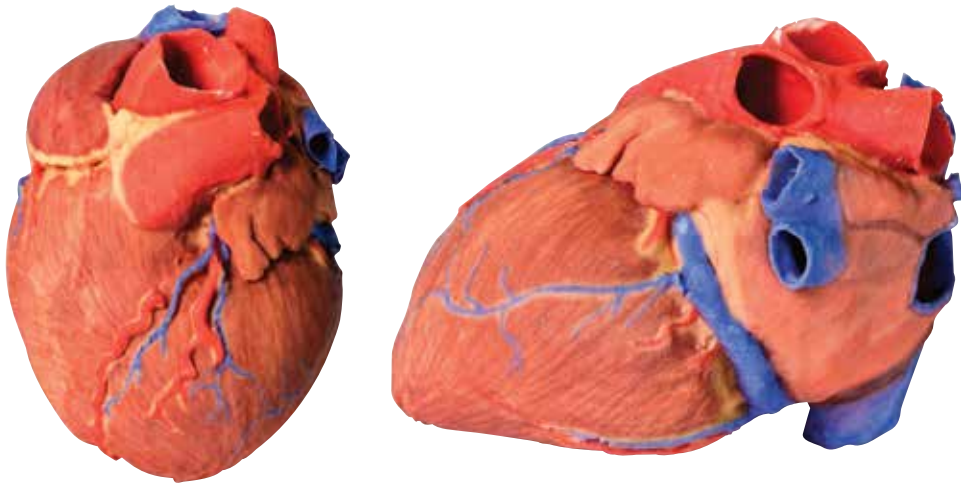
The posterior ethmoidal nerve (PEN) (a branch of the nasociliary nerve, CN V1) can be seen passing between the medial rectus (MR) inferiorly and the superior oblique muscle superiorly. A small piece of the orbital plate of the ethmoid bone (EB) has been retained to illustrate its path as it enters the posterior ethmoidal foramen. Other structures visible include the frontal nerve (FN), the sphenoid sinus (SS), the pituitary gland (PG) and the frontal sinus mucosal lining exposed after removal of the orbital plate of the frontal bone on the anterior roof of the orbit. The internal carotid and optic nerve are also visible within the cranium.



This 3D printed specimen presents the conducting pathways of the respiratory system from the trachea, carina, and complete right and left bronchial trees to the level of the tertiary lobar bronchi. Each set of lobar bronchi have been colour-coded to demonstrate the bronchopulmonary segments of the right and left lobes.

From the right primary bronchus, the secondary bronchus to the upper lobe gives rise to tertiary bronchi to the apical (yellow), anterior (blue) and posterior (brown) segments. The bronchus intermedius divides to supply the middle lobe (lateral [orange] and medial [pink]) segments. The lower lobe bronchus then gives rise to the tertiary bronchi of the superior (yellow) and basal (anterior [purple], posterior [orange], lateral [blue], medial [brown]) segments.

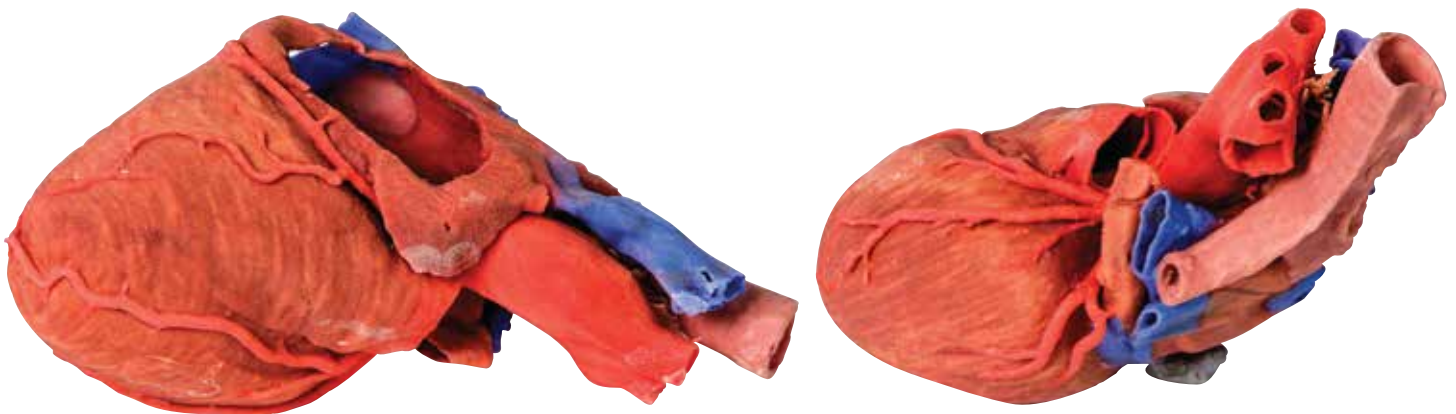
From the left primary bronchus, the secondary bronchus to the upper lobe gives rise to the tertiary bronchi to the apical-posterior (brown), anterior (blue), superior lingual (orange), and inferior lingual (pink) segments. The lower lobe bronchus gives rise to the tertiary bronchi to the superior (yellow) and basal (anteromedial [brown], lateral [orange], posterior [blue]) segments.



This 3D printed heart specimen preserves superficial cardiac anatomy and the bases of the great vessels. All four chambers (atria and ventricles) are preserved, with the pericardial reflections on the left atrium demarcating the position of the transverse and oblique pericardial sinuses.

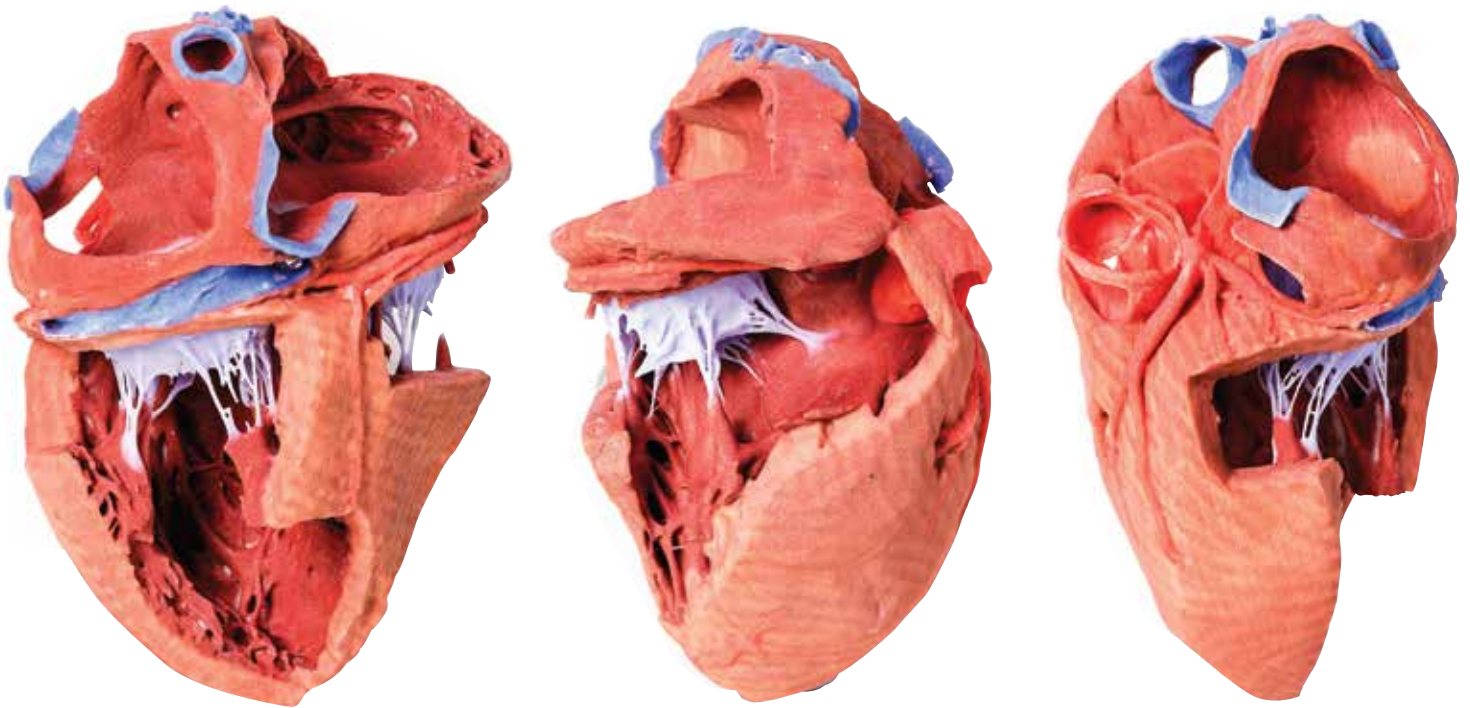
The right marginal branch of the right coronary artery is visible exiting from the fat-filled coronary sulcus, as well as the posterior interventricular (postero descending) artery within its sulcus. The anterior interventricular (left anterior descending) and diagonal branches from the left coronary artery are also visible anteriorly, as well as the terminal portion of the circumflex branch deep to the left auricle and great cardiac vein. On the posterior aspect, the coronary sinus receives all the cardiac veins (great, middle, small) and a prominent posterior vein of the left ventricle. The aortic and pulmonary semilunar valves are visible at the bases of the ascending aorta and pulmonary trunk, respectively.

Heart and the distal trachea, carina and primary bronchi MP1710



This 3D printed specimen preserves the external anatomy of the heart and the distal trachea, carina, and primary bronchi in the posterior mediastinum relative to the great vessels and left atrium (which demonstrates the pericardial reflections of the transverse and oblique pericardial sinuses).

An anterior window has been dissected into the right atrium and base of the auricle, exposing the right atrioventricular (tricuspid) valve and passage into the right ventricle. Both the right and left coronary arteries and named branches are visible (with the posterior interventricular artery arising from the right coronary artery). The left auricle has been sectioned to demonstrate the course of the circumflex artery in the coronary groove. The cardiac veins have been removed, but the coronary sinus has been retained inferior to the left atrium. The pulmonary trunk has been removed to expose the (open) pulmonary semilunar valves, while the arch of the aorta is intact to display the origins of the brachiocephalic trunk, left common carotid, and left subclavian. Adjacent to the aorta, the termination of the left and right brachiocephalic veins and azygos vein into the superior vena cava is preserved.



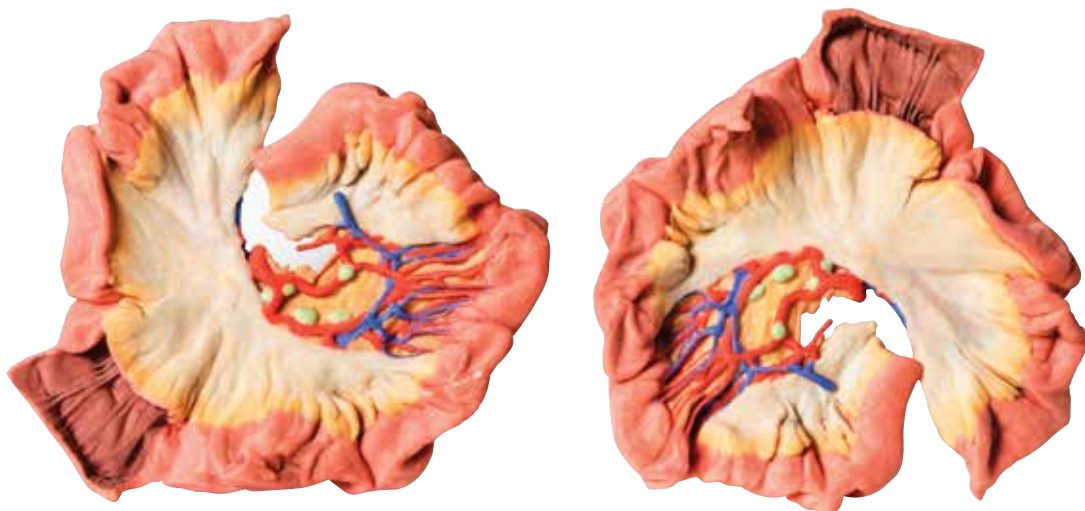
This 3D printed heart has been dissected to display the internal structures of the chambers. At the base of the heart the termination of the superior vena cava is preserved entering the right atrium. Part of the inferior vena cava is also preserved on the inferior aspect of the right atrium; however, most of the vessel lumen and much of the anterior wall has been removed to expose the pectinate muscles of the right auricle and the fossa ovalis (which is nearly translucent in the 3D print). The anterior wall of the right ventricle has also been removed to expose the right atrioventricular valve and its three cusps (anterior, posterior, and septal), including the chordae tendineae connecting them to respective papillary muscles projecting from trabeculae carneae (including a septomarginal trabecula entering the anterior papillary muscle from the interventricular septum). The smooth wall of the conus arteriosus is also exposed leading to the pulmonary semilunar valve (left, right, and anterior cusps) at the base of the pulmonary trunk. Preserved and encircling the right atrioventricular valve is the right coronary artery, ultimately passing to the posterior aspect and the origin of the posterior interventricular artery and atrioventricular nodal artery.

On the posterior side of heart the terminations of the pulmonary veins are visible entering the opened left atrium. Just anterior to the depression of the fossa ovalis in the interatrial septum the left atrioventricular valve with its two cusps (anterior and posterior) is preserved, along with the associated chordae tendineae and papillary muscles in the ventricle. The walls of the opened left ventricle preserve well-developed trabeculae carneae. At the apex of the ventricle the aortic semilunar valve (with left, right, and posterior cusps preserved) can be seen at the base of the sectioned aorta alongside the origin of both coronary arteries. The left coronary artery in this specimen is very short, giving rise almost immediately from its origin to the left anterior descending artery, the diagonal artery, the ramus intermedius, and the circumflex branch. The latter branch passes between the left atrium and ventricle adjacent to the opened coronary sinus leading to the right atrium. The left anterior descending branch penetrates the myocardium in this individual and travels through the tissue, only emerging superficially to become visible again near the apex.



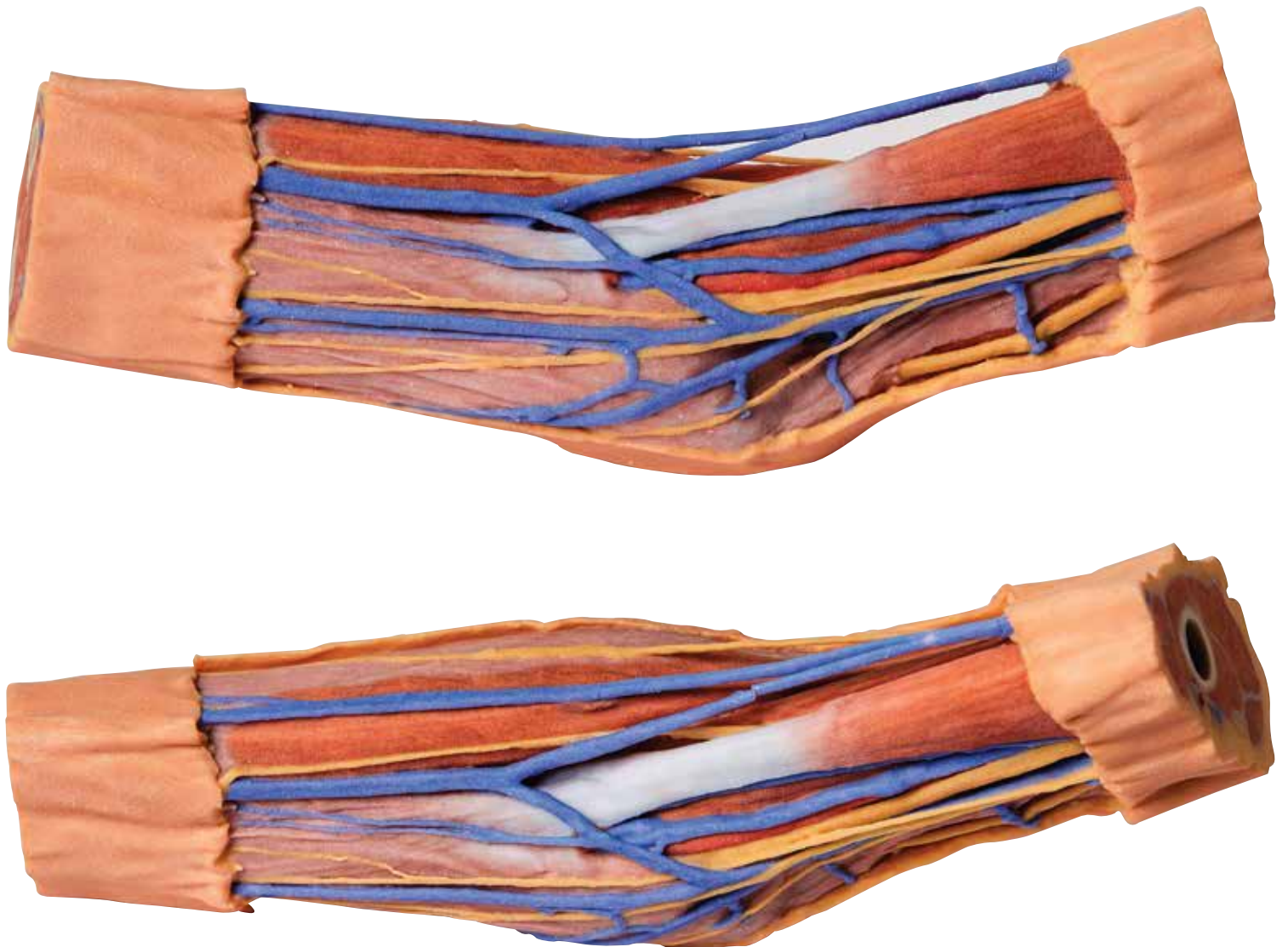
This 3D printed specimen demonstrates a small loop of ileum and mesentery. A window into the mesentery has been dissected (removing fat and visceral peritoneum) to show arterial arcades in the mesentery (many short vasa rectae and more numerous arcades than in jejunum).

There are several large lymph nodes surrounding the larger vessels near the root of the mesentery. A distinct feature of the fat in the mesentery extending up to (and indeed, beyond) the mesenteric border of the bowel. A small portion of the lumen has been opened to reveal the nature of the mucosal folding (fewer but larger folds than jejunum).



This 3D printed specimen presents a small loop of jejunum and mesentery. A window into the mesentery, fat and visceral peritoneum has been removed to illustrate the arterial arcades in the mesentery (many long straight vasa rectae and fewer vascular arcades than in ileum).

Also note the presence of lymph nodes (grey-light green) which are a prominent feature of the mesentery, especially near its root close to larger vessels. Classically the fat in the mesentery in the jejunum does not extend to the mesenteric border of the jejunum and would normally allow the observer to view the long straight vessels (vasa recti). However in this example from an individual with a reasonably large amount of abdominal fat, this 'window' is not apparent as fat extends further towards the mesenteric border of the jejunum. A small segment of the lumen of the jejunum has been opened to reveal the nature of the mucosal folding (more folds and smaller folds than the ileum).



This 3D printed cubital fossa displays a superficial dissection of the right distal arm and proximal forearm. The skin and superficial fascia has been removed anteriorly, medially and laterally to expose the superficial veins (basilic, cephalic, and median cubital) and cutaneous (medial, lateral and posterior antebrachial) nerves. The deep fascia underlying these superficial structures has been largely removed, although the antebrachial fascia has been retained medially to demonstrate the merging of connective tissue fibres with the tendon of the biceps brachii through the bicipital aponeurosis. Medially, the ulnar artery is visible entering the cubital tunnel proximal to the medial epicondyle of the humerus. Anteriorly, the median nerve, brachial artery and accompanying veins in parallel to the biceps brachii. On the lateral aspect, the cephalic vein rests on the brachioradialis muscle, and the posterior antebrachial cutaneous nerve rests on the common origin of the forearm extensor muscles (and just anterior to the exposed origin of the triceps brachii muscle).

The proximal cross-section displays the anterior and posterior arm compartment muscles (biceps brachii, brachialis, triceps brachii), neurovascular bundles (median, ulnar, radial nerves; brachial artery and veins) and superficial veins (basilic, cephalic) visible at the midshaft of the humerus. The distal cross-section displays the anterior and posterior forearm compartment muscles separated by the interosseous membrane, as well as the superficial and deep neurovascular bundles (radial artery, vein and superficial branch of the radial nerve; ulnar artery, vein and nerve; median nerve; anterior and posterior interosseous arteries, veins and nerves) and the distal continuations of the superficial veins and cutaneous nerves.



This 3D printed specimen presents a left distal arm and proximal forearm with all skin, subcutaneous fat and superficial cutaneous nerves and veins removed. The elbow region partially flexed to display the arrangement of muscles and neurovascular structures of the cubital fossa.

Viewed from the anterior aspect the most obvious feature is the biceps brachii muscle, with its insertion in the form of the flattened bicipital aponeurosis passing medially over the muscles of the common flexor origin and the more rounded tendon passing deep to insert into the radial tuberosity. The brachialis muscle lies deep to biceps brachii and is visible from the lateral aspect. In the proximal part of the forearm the brachioradialis muscle (slightly elevated and reflected laterally to reveal deeper structures) and extensor carpi radialis longus are identifiable. On the medial side one can see the classic arrangement of the biceps brachii tendon, brachial artery and median nerve (TAN) from lateral to medial. They are partially covered by the bicipital aponeurosis as they course distally. The ulnar nerve can be seen changing position from the anterior compartment of the arm to the posterior compartment (the intermuscular septum has not been preserved but triceps muscle is clearly evident) to pass behind the medial epicondyle and enter the cubital tunnel. It travels distally between the two heads of flexor carpi ulnaris. Close inspection of the groove between brachialis and brachioradialis reveals the radial nerve (which would not be visible if the brachioradialis muscle had not been partly reflected). It lies amongst some fat (yellow) but its superficial branch passes distally below brachioradialis.

In the posterior view the triceps tendon inserts into the olecranon process of the ulna. The medial and lateral epicondyles are also clearly visible (grey/white in colouration). The medial epicondyle is clearly identifiable as it has the ulnar nerve passing posteriorly before penetrating the deep fascia covering the gap between the two heads of flexor carpi ulnaris.

The proximal section through the arm reveals the biceps muscle lying anteriorly with the neurovascular bundle on its medial side which contains the brachial artery together with median nerve and ulnar nerve (veins have been removed). The three heads of triceps (lateral, long and the deeper placed medial head) are clearly visible in the posterior compartment. On the distal section through the forearm it is more difficult to discern each muscle, but the cut surfaces of the radius and ulna are clearly visible - as is the brachial artery lying medial to pronator teres muscle and the median nerve lying just deep to this muscle (which is the most lateral of the muscles arising from the common flexor origin).

Male left pelvis and proximal thigh MP1765



This 3D printed male left pelvis and proximal thigh (sectioned through the midsagittal plane in the midline and transversely through the L3/4 intervertebral disc) shows superficial and deep structures of the true and false pelvis, inguinal and femoral region. In the transverse section, the epaxial musculature, abdominal wall musculature (rectus abdominis, external and internal abdominal obliques, transversus abdominis), psoas major and quadratus lumborum are visible and separated from each other and the superficial fat by fascial layers such as the rectus sheath and the thoracolumbar fascia. The psoas major muscle lies lateral to the external iliac artery, with the left testicular artery and vein lying on its superficial surface. More laterally (and moving inferiorly), the ilioinguinal nerve, the lateral cutaneous nerve of the thigh and the femoral nerve are positioned over the superficial surface of the iliacus muscle.

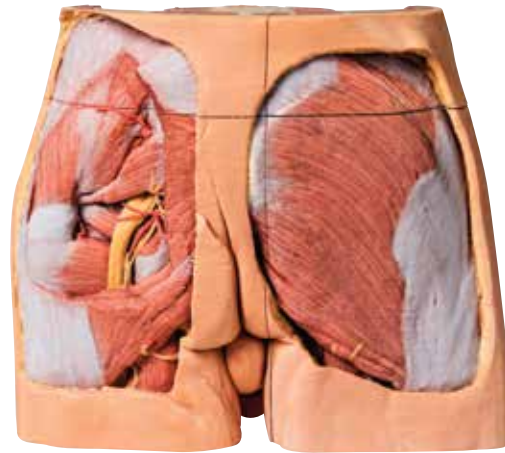
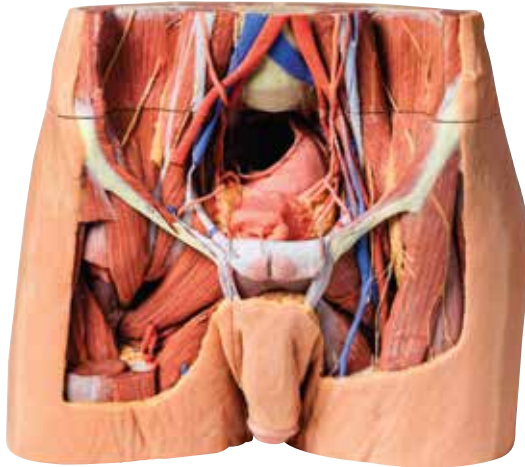
The left common iliac artery bifurcates at the level of the sacral promontory into the external and internal iliac arteries. This specimen does not possess a clearly defined anterior and posterior division of the internal iliac artery; instead, the terminal arteries sequentially radiate from the internal iliac. The lateral sacral, inferior rectal, inferior gluteal, internal pudendal, superior vesical, obturator and umbilical arteries (which terminates in the medial umbilical ligament) are visible adjacent to the sacral ventral rami. The inferior gluteal and

internal pudendal arteries have not bifurcated in this view and track inferiorly over piriformis.

The deep circumflex iliac artery and vein can be seen passing deep posterior to the inguinal ligament, while the branches from the inferior epigastric artery and veins can be seen perforating rectus abdominis and the overlying rectus sheath. The left common iliac vein lies deep to the left common iliac artery; the obturator branch and the external iliac vein have been preserved.

In the midline the pubic symphysis and sagittal sections of the pelvic viscera are visible: from anterior to posterior, the bladder (receiving the left ureter, which passes over the iliac vessels at the level of the pelvic brim), the left seminal vesicles and vas deferens, and rectum (with surrounding external anal sphincter muscle). The pathway of the urethra is visible from the inferior pole of the bladder through the prostate gland, pelvic diaphragm and the corpus spongiosum of the penis. Inferior to the sectioned erectile bodies (corpus cavernosa and corpus spongiosum) lies the scrotum, where the skin has been removed to reveal the parietal tunica vaginalis.

On the preserved proximal thigh the fascia lata has been removed to highlight the transition of the neurovasculature and musculature from the pelvic region. Superior to the inguinal ligament a window has been cut to reveal the underlying aponeurosis of the transversus abdominis muscle. From medial to lateral, the femoral vein and artery have been removed from the femoral sheath, and the termination of the femoral nerve lies superficial to the iliopsoas muscle. The great saphenous vein can be seen coursing medially over the pectineus, adductor longus and gracilis muscles, while branches of the femoral nerve pass over the profunda femoris artery. The thigh musculature is visible, with the cut sartorius muscle overlying the iliacus muscles and the origins of anterior thigh muscles (rectus femoris, vastus lateralis, vastus intermedius, vastus medialis). The tensor fasciae latae can be seen inserting on the anterior border of the iliotibial tract, which extends over the lateral surface of the thigh. A window has been cut to expose the underlying gluteus medius muscle, which terminates at the lateral aspect of the greater trochanter.



This 3D print specimen preserves a series of features of the head and visceral column of the neck:

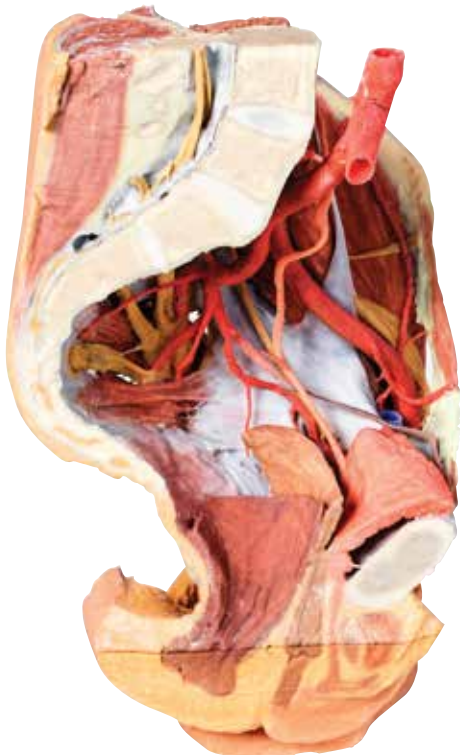
The face: On the right side of the head the parotid gland has been removed to reveal the facial nerve and all its branches (temporal, zygomatic, buccal, marginal mandibular and cervical) and demonstrate the spatial relations of structures embedded in the gland from superficial to deep (facial nerve, retromandibular vein, external carotid artery). In the surrounding region the temporalis, masseter and posterior belly of digastric are exposed, as are and the facial artery, transverse facial artery and superficial temporal artery. The facial vein and transverse facial vein are clearly visible uniting to form the common facial vein which is joined by the retromandibular vein to form the external jugular vein.

Viewed from the anterior aspect the face has been dissected to display some of the facial muscles around the mouth (buccinator [on the left], orbicularis oris and zygomaticus major). On the left side of the infratemporal fossa has been open to expose the medial and lateral pterygoids. The lateral pterygoid is divided to show the mandibular division of the trigeminal nerve dividing into the lingual nerve and the inferior alveolar branch. Also on the left side the branches of the ophthalmic division of the trigeminal that supply the skin above the eyebrows and scalp (supraorbital [left only] and supratrochlear nerves [both sides]) are dissected. The submandibular gland is clearly visible below the mandible on both sides as are the facial arteries and veins as they course over the mandible. The neck: The musculoskeletal portion of the neck have been removed to display the pharynx posteriorly, the larynx anteriorly, and the neurovascular bundles laterally. The suprahyoid and infrahyoid muscles can be seen on the neck, as well as the cricothyroid muscle. When looking up the length of the trachea from below, the vocal folds are visible. The hypoglossal nerve can be seen winding around the lateral surface of the external carotid artery and the external branch of superior laryngeal nerve is seen descending in the neck.

The internal jugular vein, the common carotid artery and its bifurcation into external and internal carotid arteries are clearly seen on both left and right. The vagus nerve in the carotid sheath is also visible. The ansa cervicalis is visible emerging below the digastric muscle and descending on the surface of the internal jugular vein. The internal branch of the superior laryngeal nerve can be seen below the superior thyroid artery on the left. The superior thyroid artery branching from the external carotid artery is seen descending in the anterior neck. The internal branch of the superior laryngeal artery is visible on the left piercing the thyrohyoid membrane above the inferior constrictor where this muscle is attached to the hyoid bone.

Posterior view of the pharynx: The superior, middle and inferior pharyngeal constrictors are indicated on the pharynx wall. The oesophagus can be identified emerging from the lower end of the pharynx. The posterior horn of the hyoid bone acts as a useful landmark. The carotid sheath seen from behind clearly shows the vagus nerve and its pharyngeal branches on the left. The recurrent laryngeal nerve is briefly visible on the left lying medial to the inferior thyroid artery. The occipital arteries are visible as they curve around the mastoid process. The vertebral arteries are seen either side of the brainstem as they enter the foramen magnum. The cerebellum has been removed to allow the fourth ventricle to be exposed. The cut surfaces of the cerebellar peduncles are clearly visible. A large portion of the posterior inferior cerebellar artery on the right is still visible as it winds around around the brainstem.

Cranial Cavity: The left and right orbits have been opened to reveal the orbital nerves and vessels along with the eyes and optic nerves. The optic chiasm, optic tracts and the lateral geniculate bodies are retained thus showing a large part of the visual pathways. The brainstem is cut at the level of the superior colliculi on the left and slightly lower on the right. The olfactory tracts and bulbs are also demonstrated. The origins of many of the cranial nerves from the brainstem are clearly visible.



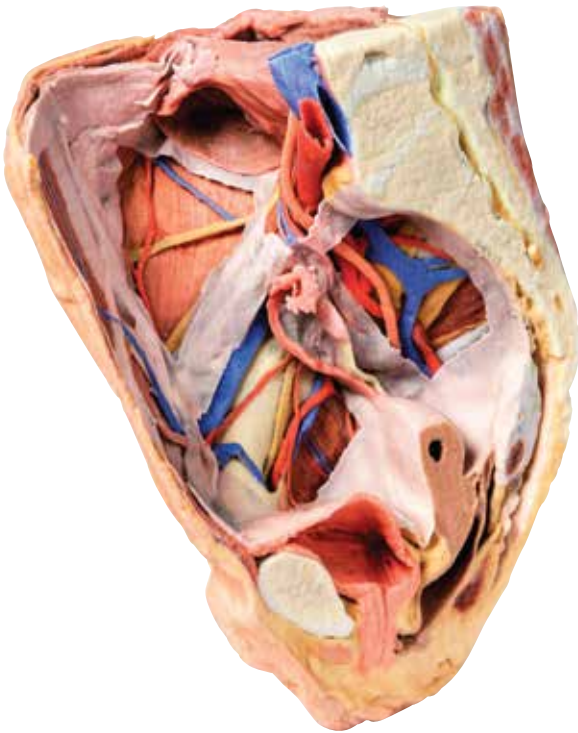
This 3D printed female left pelvis and proximal thigh preserves both superficial and deep structures of the true and false pelvis, inguinal region, femoral triangle, and gluteal region. The specimen has been sectioned transversely through the fourth lumbar vertebra, displaying the cross-section of the musculature (epaxial musculature, psoas and quadratus lumborum muscles) and cauda equina within the vertebral canal. The ventral and dorsal roots of the cauda equina are also visible exiting the intervertebral and sacral foramina in the sagittal section.

The abdominal aorta is preserved from the fourth lumbar vertebra to the bifurcation into the common iliac arteries; the root of the inferior mesenteric artery, lumbar arteries, and median sacral artery are also preserved. At the level of the sacral promontory, the common iliac artery bifurcates into the external and internal iliac arteries. Superficial to the sacral ventral rami the major branches of the internal iliac artery are visible (iliolumbar, lateral sacral, superior gluteal, inferior gluteal, internal pudendal, obturator, superior vesicle, obturator, uterine). These latter arterial branches pass to the sectioned bladder (collapsed against the pubis and receiving the ureters), uterus and vagina. The pelvic viscera (bladder, uterus, vagina and rectum) are visible in the midsagittal section extending to the anterior and posterior triangles of the perineum; in the anterior triangle the sagittal section of the clitoral body and part of the corpus spongiosum are visible inferior to the pubic symphysis.

The external iliac artery passes anteriorly along the pelvic brim, giving rise to the inferior epigastric and deep circumflex iliac arteries before passing deep to the inguinal ligament. The psoas major and minor muscles pass lateral to the external iliac artery, with the femoral nerve and lateral cutaneous nerve of the thigh resting on the superficial surface of the iliacus muscle.

The fascia lata inferior to the inguinal ligament has been removed to expose the muscular borders and contents of the femoral triangle (and surrounding anterior and medial thigh musculature). The great saphenous vein is visible joining the femoral vein adjacent to the femoral artery, with the branches of the femoral nerve just overlying the deep artery of the thigh. The distal cross-section through the proximal femur displays the anterior, medial and posterior compartment musculature, neurovascular bundles (femoral artery and vein, deep artery of the thigh, and the sciatic nerve), and tributaries of the great saphenous vein.

Posteriorly the gluteal region has been dissected to demonstrate deep structures. The gluteus maximus and gluteus medius muscles have been removed exposing the piriformis muscle. Superior to piriformis the superior gluteal artery and nerve pass laterally towards the gluteus minimus. Inferior to piriformis the inferior gluteal artery and nerve are visible (and pinned towards the sectioned edge of the gluteus maximus). The sciatic nerve and posterior cutaneous nerve of the thigh are also visible exiting the greater sciatic foramen inferior to the piriformis, running superficial to the lateral rotators (superior and inferior gemelli, obturator internus, quadratus femoris) and common origin of posterior thigh muscles (semitendinosus, semimembranosus, long head of biceps femoris) from the ischial tuberosity. The sacrotuberous ligament has been sectioned to show the internal pudendal artery and pudendal nerve exiting the greater sciatic foramen to wrap around the sacrospinous ligament and coccygeus muscle to enter the lesser sciatic foramen. The fat of the ischioanal fossa has been removed to demonstrate the course of these vessels in the perineum just lateral to the levator ani and external anal sphincter muscles.



This 3D printed female right pelvis preserves both superficial and deep structures of the true and false pelvis, as well as the inguinal ligament, the obturator membrane and canal, and both the greater and lesser sciatic foramina. Somewhat unique is the removal of portions of the peritoneum (a grayish colour) to create 'windows' displaying extraperitoneal structures.

The specimen has been sectioned transversely through the L4 vertebra, displaying a cross section of the colon, the epaxial musculature (psoas and quadratus lumborum muscles), and the abdominal wall musculature. The common iliac artery has been preserved from the level of the L4 vertebra, and its bifurcation into the external and internal iliac arteries can be observed at the level of the sacral promontory. Deep to the arteries the common iliac vein and the origin of the inferior vena cava are visible.

The external iliac artery and vein passes anteroinferiorly along the pelvic brim, giving rise to the inferior epigastric and deep circumflex arteries and veins before passing deep to the inguinal ligament. The psoas major muscle lies lateral to the external iliac artery, with the femoral nerve evident on its lateral margin close to the inguinal ligament. The lateral cutaneous nerve of the thigh travels laterally on the superficial surface of the iliacus muscle to exit the 'false' pelvis close to the anterior superior iliac spine.

Following the course of the internal iliac artery deep to the undissected peritoneum, many of the major branches of its anterior and posterior divisions can be identified. The anterior division divides (deep to the peritoneum) into the superior vesical, obturator and obliterated umbilical artery. With a course parallel to the obturator artery, the obturator nerve can be seen running over obturator internus before entering the obturator canal together with the obturator vein (nerve, artery, vein in that order from superior to inferior).

Branches of the posterior division of the internal iliac artery, iliolumbar, and several lateral sacral arteries, can be seen arising from the posterior aspect of the internal iliac just below the sacral promontory. Its terminal branch, the superior gluteal, usually passes posteriorly between the lumbosacral trunk and S1 nerve, but this is hidden from view. The internal iliac vein and its tributaries - the obturator veins, uterine vein, vesical veins, etc. can be seen lying internal to the nerves and muscles. The large S1 and S2 roots and the smaller S3 nerve root can be seen emerging from the sacral foramina to pass laterally where it is joined by the lumbosacral trunk (L4 and L5 roots) which is not visible, to form the sciatic nerve which exits through the greater sciatic foramen to emerge on the posterior aspect in the gluteal region. In the pelvis as these roots pass laterally they are interdigitated between the fibres of piriformis muscle.

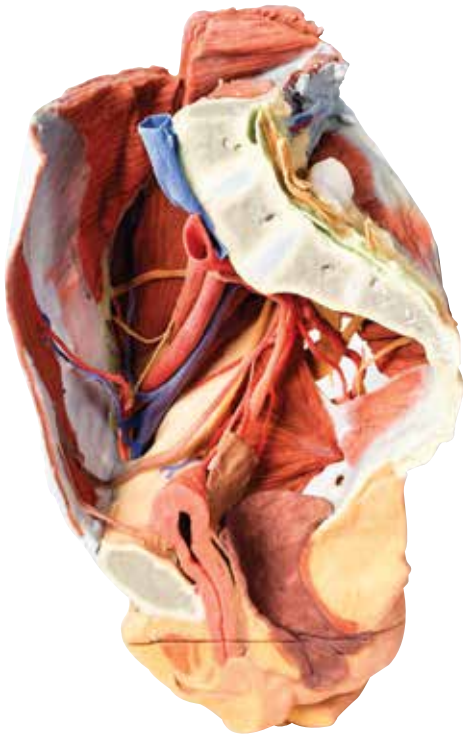
The right ureter can be clearly seen as it passes inferiorly on the posterior abdominal wall superficial to psoas muscle. It passes over the pelvic brim at the bifurcation of the common iliac artery to descend on the lateral wall of the pelvis before passing medially in the base of the broad ligament (hidden from view as the peritoneal folds that 'drape' over the uterine [Fallopian] tubes are still intact) to reach the lateral angles of the bladder.

In the pelvis the viscera which lies most anteriorly is the bladder. Its thick wall and cavity is easily seen in this mid-sagittal cut. Indeed the ureteric orifice can be seen at the angle of the trigone of the bladder on its internal mucosal surface. The relations of the uterus to the vagina are clearly visible in the mid-sagittal section. Indeed the anterior and posterior fornices are clearly seen as is the os of the cervix. The round ligament of the uterus has been removed along with some peritoneum to display the structures in the lateral pelvic wall. The entire right Fallopian tube is identifiable as it passes from the lateral aspect of the body of the uterus to terminate as the fimbria which overhangs the right ovary which is still held in place by its mesovarium. The ovary is attached laterally to the pelvic brim by the suspensory ligament of the ovary (sometimes called the infundibulopelvic ligament) which contains its named artery and veins. The ligament of the ovary is clearly visible leading from the medial aspect of the ovary to the lateral surface of the uterus.

Female right pelvis - superficial and deep structures MP1783

There are only small cut surfaces of the rectum (visible as little islands of mucosa) visible on the sagittal cut surface suggesting that it is slightly off the midline plane. Some pararectal lymph nodes (coloured pale green) can be seen close to these islands of rectal mucosa. On the anterior aspect of the 3D print the inguinal ligament has been retained and deep to it the femoral artery, vein and nerve pass to the anterior compartment of the thigh.

In the gluteal region (note the femur has been removed to expose the acetabulum) the sciatic nerve can be seen emerging from the greater sciatic foramen (GSF) alongside the inferior gluteal vessels below the remains of the piriformis fibres, whereas the superior gluteal vessels and nerve emerges above the piriformis. Below these vessels the pudendal nerves and vessels can be seen exiting the GSF and passing over the sacrospinous ligament to enter the lesser sciatic foramen, thereby entering the perineum along the lateral wall of the ischioanal fossa.



This 3D printed specimen represents a female right pelvis, sectioned along the midsagittal plane and transversely across the level of the L4 vertebrae and the proximal thigh. The specimen has been dissected to demonstrate the deep structures of the true and false pelvis, the inferior anterior abdominal wall and inguinal region, femoral triangle and gluteal region.

Internal anatomy

The muscular boundaries of the inferior abdominal cavity are defined posterolaterally by the quadratus lumborum, iliacus and psoas muscles; anteriorly by the (variably exposed) external and internal abdominal oblique muscles, the transversus abdominis and rectus abdominis. Inferiorly in the pelvic cavity, the obturator internus is visible traversing through the lesser sciatic foramen inferior to the sacrospinous ligament. Fibres of coccygeus merge with those of the sacrospinous ligament. Piriformis has been sectioned, with both origin visible within the cavity (and part visible in the gluteal region). The common iliac artery arises from its cut edge at the level of L5, bifurcating at the level of the sacral promontory into the external and internal iliac arteries. The external iliac artery crosses the pelvic brim to give off the deep circumflex iliac artery and inferior epigastric artery before exiting the pelvis deep to the inguinal ligament. The internal iliac artery runs posterolaterally, giving the iliolumbar artery posteriorly and lateral sacral arteries which enter the anterior sacral foramina. A radicular artery entering the anterior foramina of the coccyx can also be seen. Inferiorly, the

superior gluteal artery, inferior gluteal artery and internal pudendal artery exit the pelvic cavity through the greater sciatic foramen. A branch from the inferior gluteal artery, supplying psoas, travels anteriorly along the pectineal line. Anteriorly, the umbilical artery gives off the superior vesical artery (supplying the bladder) before terminating against the anterior abdominal wall as the medial umbilicalligament. Posteriorly, the inferior vesical artery arises from the obturator artery before exiting the pelvis through the obturator canal. The uterine artery crosses over the ureter to enter the remnants of the broad ligament. The major veins preserved are the inferior epigastric vein and deep circumflex iliac vein draining into the external iliac vein, and the iliolumbar vein and lateral sacral vein draining into the internal iliac vein. The external iliac vein and internal iliac vein unite to form the right common iliac vein which, at the level of L5, joins the (cut edge) of the left common iliac vein to become the inferior vena cava. Two veins pass horizontally across iliacus and quadratus lumborum.

Of the peripheral nerve structures preserved in this specimen, the lateral femoral cutaneous nerve passes laterally across the superficial aspect of the iliacus muscle and the femoral nerve is visible deep to the psoas major muscle. The genitofemoral nerve lies on the superficial surface of the psoas major, and the course of the genital branch entering the deep inguinal ring and the femoral branch passing deep to the inguinal ligament can be followed. The obturator nerve is also seen passing from deep to the psoas muscle anteriorly to the obturator foramen. In the true pelvis the lumbosacral trunk crosses the pelvic brim and joins the anterior ramus of S1. The S1-S3 anterior rami are visible and can be followed as they pass through the greater sciatic foramen and enter the gluteal region. In addition to the muscular and neurovascular structures, parts of pelvic viscera have been preserved. Posterior to the pubic symphysis the median umbilical ligament extends superiorly from the bladder to the anterior abdominal wall. The ureter descends anteriorly to the psoas major muscle, across the iliac vessels, and beneath the uterine artery to enter the posterior bladder wall. The urethra is seen passing downwards to its opening at the urinary meatus, just posterior to the clitoris. Posterior to the bladder are the posthysterectomy remnants of the uterus at the apex of the closed, superior end of the vagina. Posterior to this part of the cut rectum, anal canal and anus are present. Some muscular fibres of levator ani and the external anal sphincter can be seen in the ischioanal fossa just posteriorly to the anal canal.

External anatomy

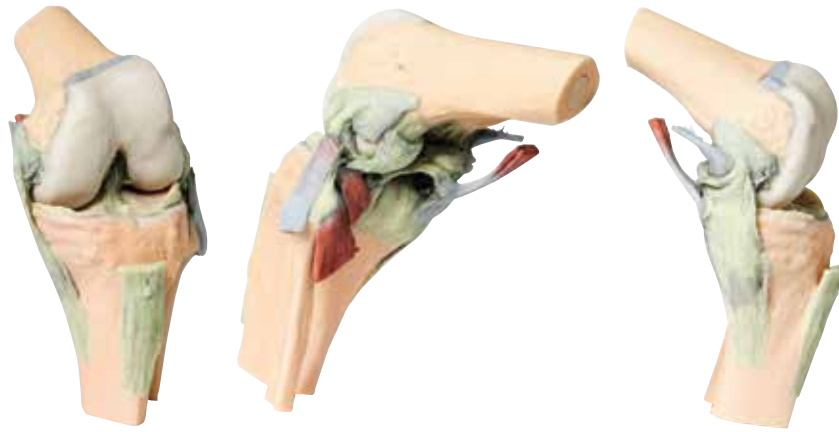
In the posterior view, most of the multifidus and origin of the gluteus maximus have been removed over the lumbar and sacral region, and

the laminae of L4 and L5 and the dorsal sacrum have been sectioned to reveal the cauda equina in the vertebral and sacral canal. The dura mater has been partially sectioned to expose the roots traversing the region, including the passage of the sacral ventral rami through the ventral foramina. Laterally, a large window into the gluteal maximus has been opened to expose the deeper structures of the gluteal region. Part of the sectioned piriformis is visible in the greater sciatic foramen, with the sciatic nerve (preserving an early division of the common peroneal and tibial nerves within the gluteal region) surrounded by the superior and inferior gluteal arteries. The sectioned internal pudendal artery and pudendal nerve rest on the sacrotuberous ligament as they descend towards the lesser sciatic foramen. Inferior to the sacrotuberous ligament the obturator internus muscle (along with the superior and inferior gemelli muscles) passes laterally deep to the common peroneal and tibial nerves. Inferior to these lateral rotators, the quadratus femoris and common origin of the hamstring group are visible just proximal to the remaining portion of the gluteus maximus.

In the anterior view, a window has been cut into the aponeurosis of the external oblique aponeurosis to reveal part of the transversus abdominis muscle. The inguinal ligament can be seen arising from the anterior superior iliac spine and extending towards the pubic tubercle. Inferior to the inguinal ligament, the fascia lata has been removed over the anterior thigh. The visible thigh muscles (from lateral to medial) on this specimen include the tensor fasciae latae, and those of the anterior (sartorius, rectus femoris and the iliopsoas) and medial (gracilis, pectineus [sectioned], obturator externus, adductor brevis, adductor longus and adductor magnus).

Between these muscle groups the femoral sheath has been removed to expose the contents of the femoral triangle (femoral artery and vein; sectioned to display the deeper adductor muscle fibers) and the femoral nerve that have entered this region deep to the inguinal ligament. In this individual the lateral circumflex femoral artery arises directly from the femoral artery. Inferior to this, the deep femoral artery (profunda femoris) branches off. Several anastomosing veins draining into the femoral vein surround the deep femoral artery. The femoral vein preserves an opening on the medial side corresponding to the drainage point of the great saphenous vein. The medial circumflex artery, posterior branch of the obturator nerve and a muscular artery can be seen passing just superficial to obturator externus. The anterior branch of the obturator nerve can be seen more anteriorly, passing superficial to adductor magnus and deep to adductor longus. The sectioned thigh of the specimen allows for orientation of muscles and neurovascular structures in the proximal thigh. Other than the relations of anterior, medial and posterior thigh muscles, perforating arteries and veins are visible near the adductor magnus; and the common peroneal and tibial nerves are visible in the posterior compartment.

Flexed knee joint MP1800



This 3D printed specimen demonstrates the ligaments of the knee joint with the leg in flexion. In the anterior view, with the patella and part of the patellar ligament removed, the medial and lateral menisci and anterior and posterior cruciate ligaments are visible. Both tibial and fibular collateral ligaments are intact.

Medially, the insertions of the adductor magnus and semimembranosus muscles are retained, with the oblique popliteal ligament reflected onto the posterior aspect of the joint capsule. Laterally, the insertion of the biceps femoris and origins of the popliteus and soleus muscles have been preserved.

Knee joint extended MP1805



This 3D printed specimen demonstrates the ligaments of the knee joint with the leg in extension; it represents the same specimen as MP1807 knee joint printed in a flexed position.

In the anterior view, with the patella and part of the patellar ligament removed. Both tibial and fibular collateral ligaments are intact. Medially, the insertions of the adductor magnus and semimembranosus muscles are retained, with the oblique popliteal ligament reflected onto the posterior aspect of the joint capsule. Laterally, the insertion of the biceps femoris and origins of the popliteus (covered by the arcuate popliteal ligament) and soleus muscles have been preserved.



This 3D printed specimen displays a deep dissection of a left knee joint with the internal joint capsule structures relative to superficial tissues in a flexed position. The proximal cross-section through the distal thigh captures a small portion of the quadriceps femoris and sartorius anteriorly (with the thickened connective tissue of the iliotibial tract), the fat-filled popliteal fossa (with the popliteal vessels, tibial and common peroneal nerves), and the termination of the medial (adductor magnus tendon, gracilis) and posterior thigh muscles (biceps femoris, semitendinosus, semimembranosus) posteriorly. The distal cross-section through the leg preserves the most proximal portion of the muscles of the anterior, lateral and posterior compartments. Also visible in the section are the associated neurovascular structures: the anterior tibial artery, vein and deep peroneal nerve; the posterior tibial artery, vein and tibial nerve; and the fibular artery and vein.

Anteriorly, the skin, subcutaneous tissue and patella have been removed, with only remnant portions of the tendon of the quadriceps femoris and patellar ligament retained. With the joint capsule opened, the anterior and posterior cruciate ligaments and the menisci are visible positioned between the femoral condyles and tibial plateau. On the medial aspect, the tibial (medial) collateral ligament passes just anterior to the insertion of the semitendinosus of the pes anserinus (the sartorius and gracilis tendons are sectioned), which in turn is just anterior to the posterior compartment musculature (covered by crural fascia). On the lateral aspect, the fibular (lateral) collateral ligament is preserved, and the anterior crural musculature is exposed. Passing from the thigh are the inserting tendon of the biceps femoris onto the head of the fibula, as well as the common peroneal nerve.



This 3D printed specimen preserves a superficial dissection of the lower limb musculature from the mid-thigh to mid-leg, as well as nerves and vessels of the popliteal fossa. The insertions of the muscles of the anterior, middle and posterior compartments of the thigh are visible, including the pes anserinus medially and the iliotibial tract laterally. The capsule of the knee joint has been opened anteriorly to demonstrate the menisci and the tibial and fibular collateral ligaments. The superficial muscles of the leg are visible, with the anterior and lateral compartment muscles highlighted deep to the crural fascia. Within the popliteal fossa, both the popliteal artery and vein are visible descending from the adductor hiatus. The sciatic nerve is seen bifurcating in the fossa, with the common fibular, tibial, and sural nerves preserved.

The proximal cross-section provides a view of the distal thigh musculature of the anterior, medial and posterior compartments. The femoral artery and vein and saphenous nerve are visible within the adductor canal. The sciatic nerve and perforating branches of the profunda femoris artery (and accompanying veins) are visible in the posterior compartment. In the distal cross-section, muscles of the anterior, lateral and posterior compartment are visible. The superficial and deep fibular nerves are visible in the anterior and lateral compartments, respectively. In the anterior compartment, the deep fibular nerve is adjacent to the anterior tibial artery and veins. In the posterior compartment, deep to soleus, both the posterior tibial and fibular arteries and veins are highlighted near the tibial nerve.



This 3D printed specimen presents a deep dissection of a left pelvis and thigh to show the course of the femoral artery and sciatic nerve from their proximal origins to the midshaft of the femur. Proximally, the pelvis has been sectioned along the mid-sagittal plane and the pelvic viscera are removed. In the pelvis the coccygeus muscle spans between the sacrum and iliac spine and the obturator artery and nerve entering the obturator canal superior to the obturator membrane. The lumbosacral trunk is visible descending to join the S1-S3 ventral rami to form the sciatic nerve. The nerve exits the pelvis via the greater sciatic foramen (defined by the preserved sacrotuberous and sacrospinous ligaments) and passes superficial to the preserved gluteus minimus, piriformis, obturator internus, superior and inferior gemellus, and quadratus femoris muscles. The posterior compartment muscles of the thigh have been dissected to demonstrate the course of the sciatic (and constituent tibial and common peroneal components) as it descends towards the popliteal fossa.

Just lateral to the lumbosacral trunk in the pelvis are the iliacus and (partial) psoas muscles, as well as the proximal portion of the rectus femoris. The femoral artery is preserved as it crosses the superior pubic ramus, giving rise to the superficial circumflex iliac and superficial epigastric arteries as they enter the proximal thigh. As the femoral artery crosses through the femoral triangle, the medial and lateral circumflex femoral arteries arise and are distributed through the medial and anterior compartment; including several branches entering the preserved vastus lateralis muscle. The profunda femoris (deep artery of the thigh) also arises proximally and descends giving off perforating branches to the posterior thigh muscles. The removal of the anterior and posterior thigh muscles provides a view of the femoral artery passing across the superficial surface of the adductor muscles and exiting the femoral triangle. The obturator externus muscle also passes from the anterior surface of the obturator membrane towards the trochanteric fossa of the greater trochanter.



This 3D printed specimen presents a superficial dissection of a left lower limb, from just proximal to the knee joint to a complete foot.

The skin and superficial fascia have been removed to display the superficial venous structures of the leg including the dorsal venous plexus, great saphenous vein (including numerous tributaries), and the small saphenous vein (including numerous tributaries) on the crural fascia. Accompanying these venous structures are several cutaneous nerves, including the sural nerve posteriorly, the saphenous nerve medially, and the superficial peroneal nerve anteriorly. On the dorsum of the foot, and lateral to the tendon of the extensor hallucis longus muscle passing over the first metatarsal towards the hallux, the dorsal digital branch of the deep peroneal nerve is visible emerging to supply the skin between the first two pedal digits.



This 3D printed specimen preserves the distal thigh and proximal leg, dissected posteriorly to demonstrate the contents of the popliteal fossa and surrounding region. The proximal cross-section demonstrates the anterior, posterior and medial compartment muscles, with the origin of the popliteal artery and vein just as they have entered the popliteal fossa via the adductor hiatus. The sciatic nerve and great saphenous vein are also visible. The skin, superficial fascia, fascia lata and crural fascia has been removed posteriorly to demonstrate the course of the popliteal vessels, tibial nerve and common peroneal nerve. Medially, the semitendinosus and semimembranosus muscles have been sectioned to demonstrate the superior medial genicular artery and the medial head of the gastrocnemius. Distally, the medial gastrocnemius itself has been sectioned to expose the popliteus muscle and the tendon of the plantaris muscle.

The course of the popliteal artery and vein can be traced through the fossa to the passage of the vessels deep to soleus. They are accompanied by the tibial nerve, with the lateral head of the gastrocnemius removed several muscular branches of the tibial nerve are visible in the fossa (as is the medial sural cutaneous nerve and the distal-most part of the lateral sural cutaneous nerve). Running in parallel, the common peroneal descends and passes laterally over the exposed soleus muscle to the neck of the fibula just distal to the attachment of the biceps femoris muscle. Deep to the biceps femoris, the superior lateral genicular branch can be observed passing towards the anterior compartment. The distal cross-section demonstrates the continuation of popliteal contents and branches. The great saphenous vein, small saphenous vein and sural nerves are visible within the superficial fascia. Between the muscles of the posterior, lateral, and anterior compartments are the neurovascular bundles of the leg (posterior tibial artery, veins and tibial nerve; peroneal artery and veins; anterior tibial artery, veins and deep peroneal nerve).



This 3D printed specimen preserves the distal thigh and proximal leg, dissected posteriorly to demonstrate the contents of the popliteal fossa and surrounding region. The proximal cross-section demonstrates the anterior, posterior and medial compartment muscles, with the femoral artery and vein visible within the adductor canal. The sciatic nerve and great saphenous vein are also visible.

The skin, superficial fascia, and deep fascia have been removed over the popliteal fossa to expose the contents of the space. The muscular borders of the space are intact except for a window cut into the semimembranosus muscle to allow a view of the popliteal artery and vein near the adductor magnus. On the medial aspect of the window the great saphenous vein descends on the surface of the sartorius muscle. Distally the sartorius is visible joining the semitendinosus and semimembranosus muscles to form the pes anserinus. All major deep and superficial nerves and vessels of the space are visible, including the superior lateral genicular artery passing towards the anterior compartment of the thigh. Along the lateral margin the posterior aspect of iliotibial tract is visible descending to the lateral epicondyle of the tibia.

The distal cross-section demonstrates the continuation of popliteal contents and branches. The great saphenous and small saphenous veins are visible within the superficial fascia, as are the medial and lateral sural cutaneous nerves. Between the muscles of the posterior, lateral, and anterior compartments are the neurovascular bundles of the leg (posterior tibial artery, veins and tibial nerve; peroneal artery and veins; anterior tibial artery, veins and deep peroneal nerve; superficial peroneal nerve).



This 3D print records the anatomy of a right distal leg and the deep structures of the plantar surface of the foot. Proximally, the tibia, fibula, interosseous membrane, and leg muscles are discernable in cross-section. Medially, at the level of the ankle joint, the long tendons of the dorsi- and plantar-flexors are visible superficial to the capsular and extra capsular ligaments. The posterior tibial artery, veins, and tibial nerve are exposed through their course from the posterior leg to the plantar surface of the foot.

Laterally, the course and insertion of the fibularis muscles (longus, brevis and tertius) are visible. On the dorsum of the foot, the anterior tibial artery and deep fibular nerve emerge from deep to the extensor hallucis longus just superficial to the extensor hallucis brevis and extensor digitorum brevis muscles. On the plantar surface of the foot, the plantar aponeurosis and portions of the superficial and deep musculature (flexor digitorum brevis, abductor hallucis, abductor digiti minimi, quadratus plantae) has removed between the calcaneous and bases of the metatarsals to display the course of the tibialis posterior, flexor digitorum longus, flexor hallucis longus, and fibularis longus tendons. The origins of both the flexor hallucis brevis and flexor digiti minimi brevis are visible, as are lumbricals arising from the flexor digitorum longus tendons.



This 3D printed specimen is a left foot with superficial structures exposed on the dorsum, and the superficial layer of muscles and nerves on the plantar surface.

The anterior portion of the plantar aponeurosis has largely been removed to expose the first layer of muscles. A small portion of the lateral band of the plantar aponeurosis is preserved with the attachment to the fourth metatarsal visible. The flexor digitorum brevis muscle and tendons overlie the flexor digitorum longus tendon, although both the divisions of the tendon and the lumbricals muscles are visible approaching the flexor sheaths. The superficial branches of the medial and lateral plantar nerves radiate from the margins of the flexor digitorum brevis muscle, and can be seen dividing into the common and proper plantar digital branches. At the margins of the plantar dissection, both the abductors and flexors of the hallux and fifth digit are exposed, with both medial and lateral heads of the flexor hallucis brevis inserting into prominent sesamoids on either side of the flexor hallucis longus tendon.

On the dorsum, a window of skin has been removed to expose the dorsal fascia of the foot and underlying tendons from the anterior compartment of the leg. The dorsal fascia has been removed over the lateral metatarsals to expose the extensor hallucis brevis, the tendons of the extensor digitorum longus and brevis, and the dorsal interosseous muscles.

At the proximal end of the specimen, the distal tibia and fibula are visible joined by the interosseous membrane. The tendons and muscles of the leg compartment muscles are visible, including the tendocalcaneus. Both the anterior and posterior tibial arteries (with accompanying veins) are visible in cross section, as are the superficial fibular nerve and tibial nerve.



This 3D printed specimens preserves a mixed superficial and deep dissection of a left distal leg and foot. Posteriorly, the compartment muscles and neurovascular structures have been removed to isolate the tendocalcaneus and expose the body of the calcaneus. Medially, the tibialis posterior and flexor digitorum longus tendons are visible deep to the crural fascia, joined by the tendon of the flexor hallucis longus as the tendons passing deep to the flexor retinaculum (opened to demonstrate the tendon passage) to the medial foot. The adductor hallucis, medial head of the flexor hallucis brevis, and flexor digitorum brevis muscles are all exposed on the medial aspect of the foot.

On the dorsum of the foot, both superior and inferior extensor retinacula are preserved, with the muscles of the anterior compartment of the leg extending to their distal attachments (including the fibularis tertius). The anterior tibial artery is exposed through to the dorsalis pedis artery. Deep to these long tendons are the extensor hallucis brevis and extensor digitorum brevis muscles, as well as the dorsal interosseous muscles. On the lateral aspect, both fibularis longus and brevis are visible deep to the crural fascia, with their tendons passing deep to both superior and inferior fibular retinacula. On the lateral margin of the foot the abductor digit minimi muscle is exposed.



This 3D printed specimen presents both superficial and deep structures of a right distal leg and foot. Proximally, the posterior compartment of the leg has been dissected to remove the triceps surae muscles and tendocalcaneus to demonstrate the deep muscles of the compartment (tibialis posterior, flexor digitorum longus, flexor hallucis longus). Adjacent to these muscles the course of the tibial nerve and posterior tibial artery can be followed to the origin of the medial and lateral plantar branches at the level of the flexor retinaculum. The origin of the abductor hallucis brevis muscle has been removed to expose more of the artery and nerve branches.

The origin of the great saphenous vein from the medial aspect of the dorsal venous arch is preserved, with the vessel ascending to the cut edge of the specimen. Although the anterior compartment muscles have been removed to demonstrate the interosseous membrane, the course of the anterior tibial artery, and the deep fibular nerve to the dorsum of the foot; the tendinous insertions of the tibialis anterior, extensor hallucis longus, and the hallucal tendon of the extensor digitorum longus have been retained passing deep to the inferior extensor retinaculum. The anterior tibial artery is continuous through dorsalis pedis to the arcuate artery and the dorsal metatarsal arteries. The removal of the dorsal interosseous muscles demonstrate the approach of these terminal branches to the plantar interosseous muscles.

On the lateral aspect of the specimen, the fibularis longus and fibularis brevis muscles and tendons are visible, with tendons passing deep to the cut edge of the superior fibular retinaculum and complete inferior fibular retinaculum. Adjacent to the insertion of the fibularis brevis is the preserved tendon of the extensor digitorum longus to the fifth digit and the termination of the superficial fibular nerve; adjacent to the fibularis longus tendon entering the plantar surface of the foot is the origin of the abductor digiti minimi muscle.

Deep to these more superficial structures are several of the distal leg and foot ligaments, including the anterior and posterior tibiofibular ligaments, calcaneofibular ligament, dorsal and posterior talonavicular ligaments, and the deltoid ligament.



This 3D printed specimen provides a view of deep plantar structures of a right foot. Medially, the cut edge of the great saphenous vein is visible within the superficial fascia, just anterior to the cut edges of the medial and lateral plantar arteries and nerves overlying the insertion of the tibialis posterior muscle.

The superficial fascias, the plantar aponeurosis, and superficial musculature have been removed to expose the deep (third layer) of musculature. The cut edges of the first, second and third layer muscles are preserved on the calcaneus for orientation, as is the cut tendon of the flexor digitorum longus muscle descending into the foot and the exposed distal tendons of the flexor digitorum longus and brevis muscles. The transverse and oblique heads of the adductor hallucis are visible deep to the tendon of the flexor hallucis longus muscle (surrounded by a complete lateral head and partial medial head of the flexor hallucis brevis muscle). The plantar interosseous muscles are visible deep to the adductor hallucis. Deep to the musculature the ligaments of the tarsal and metatarsal joint capsules are exposed, as well as the long and short plantar ligaments and the plantar calcaneonavicular ligament. On the lateral aspect, the abductor digiti minimi muscle has been sectioned to expose the insertions of the peroneus longus and brevis tendons are exposed.



The Centre for Human Anatomy Education has been established within the Department of Anatomy & Developmental Biology to ensure that the teaching of human anatomy at Monash University in medical and allied health courses is of the highest international standard. The Centre also shows leadership in the enhancement of existing more traditional approaches to anatomy education as well as the development of novel approaches suited to the 21st Century in line with evidence based teaching practices. Promotion of cross-disciplinary, integrated and inter professional approaches to anatomy education are also encouraged. The Centre also has a mission of scholarly research not only in the area of education but also in modern areas of anatomical sciences such as the evolutionary, developmental and functional basis of human form.